TIMKEN

On the Effect of Prior Austenite Grain Size on the Rate of Ferrite Allotriomorph Growth and Final Ferrite ½ Thickness in Hypoeutectoid Fe-0.3C and Fe-0.3C-X Alloys

Alemi Meeting, McMaster University

June 18, 2007

E. Buddy Damm, Ph.D.
The Timken Company
Section Manager – Application Metallurgical Laboratory

Advanced Steel Processing and Products Research Center

TIMKEN

Outline

- Definitions
- Background and Introduction
- Questions and Outline
- Experimental Procedures
- Results and Discussion
  - Microstructural Evolution
  - Analytical Results
    - DICTRA vs. Experiment
    - Phase Field Simulations
- Conclusions and Future Work

Definitions

Allotriomorph

- Grain boundary ferrite

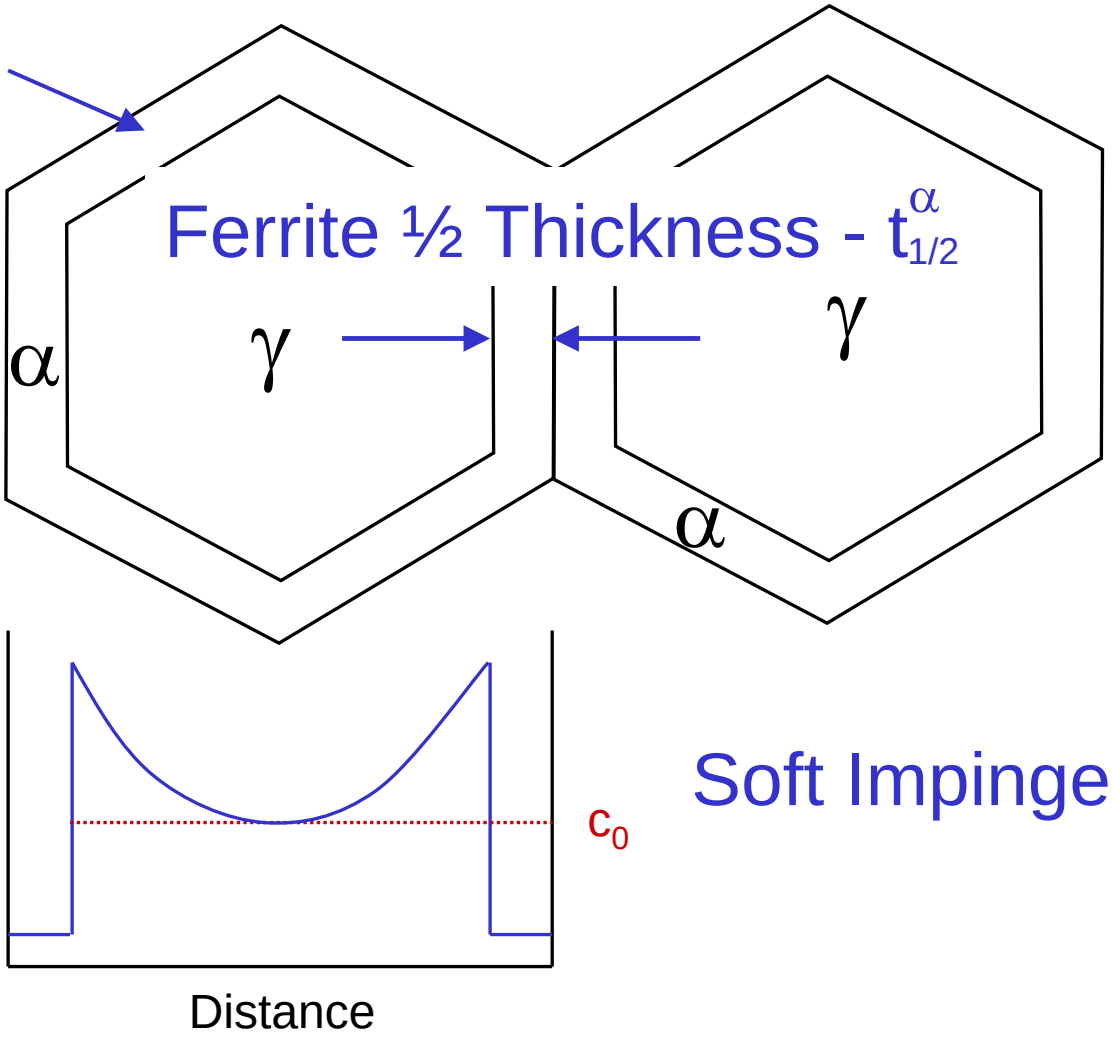

Soft Impingement

TIMKEN

DCM Vs. ICM Growth

For a fixed thermodynamic condition(s)…

DCM – Diffusion Controlled Mode

The interface mobility is effectively infinitely fast, and the rate of diffusion controls the progress of the transformation.

ICM – Interface Controlled Mode

The diffusion mobility is effectively infinitely fast, and the interface mobility controls the rate of transformation.

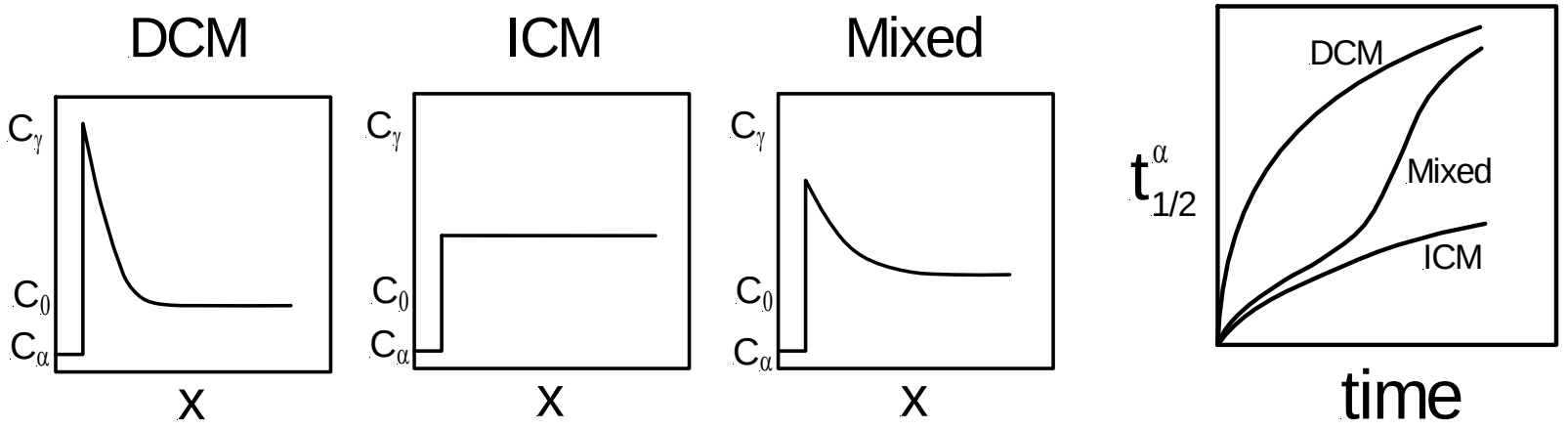

Background

Controlled Thermomechanical Processing (CTMP)*

- Measured and simulated overall transformation in medium carbon alloy steels as a function of prior austenite grain size (PAGS).

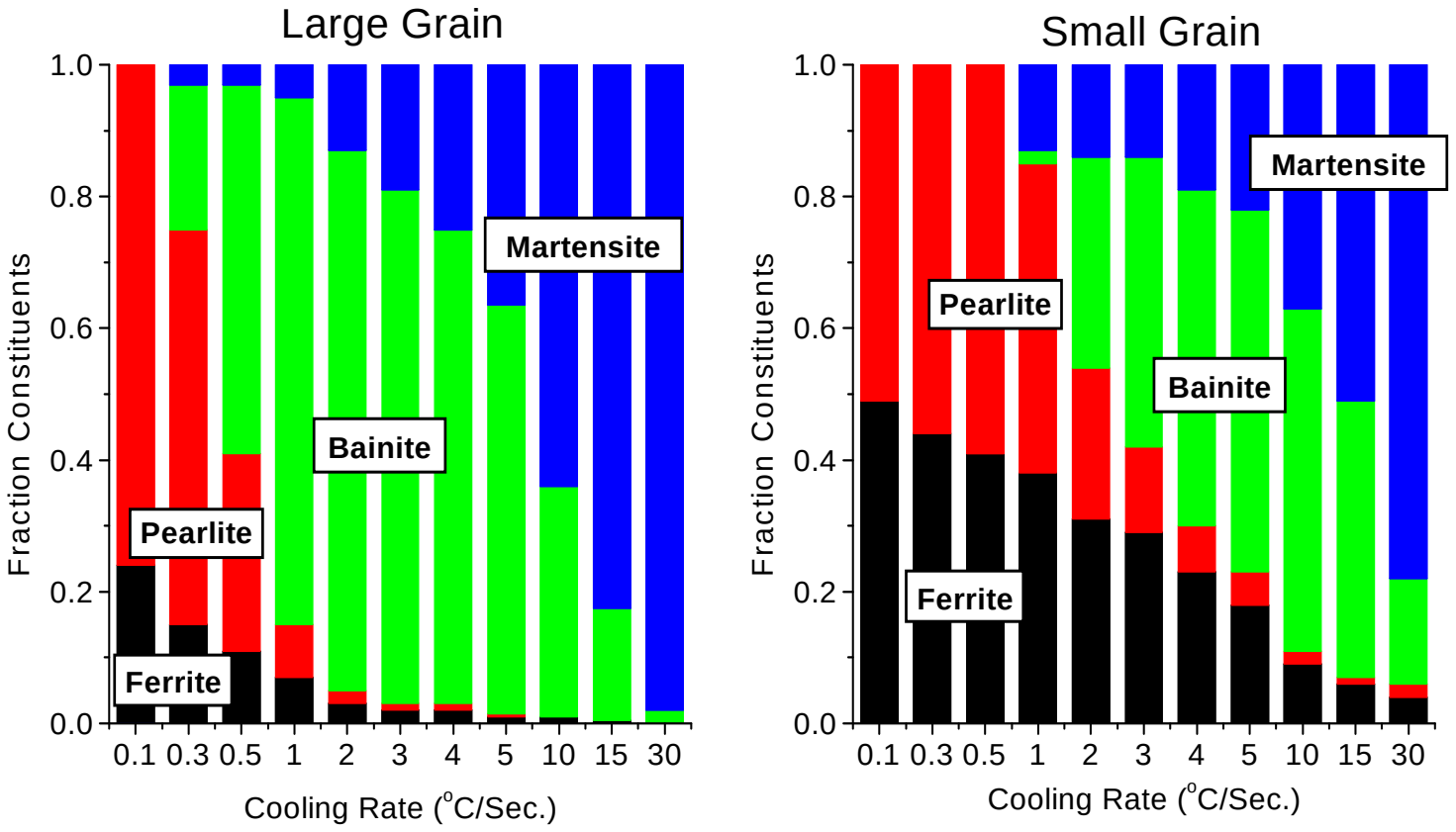

* Ref. Damm & Lusk, 2001 – DOE Contract DE-FC07-99ID13819

Advanced Steel Processing and Products Research Center

TIMKEN

Background Continued

Simple extrapolations do not accurately describe what is happening

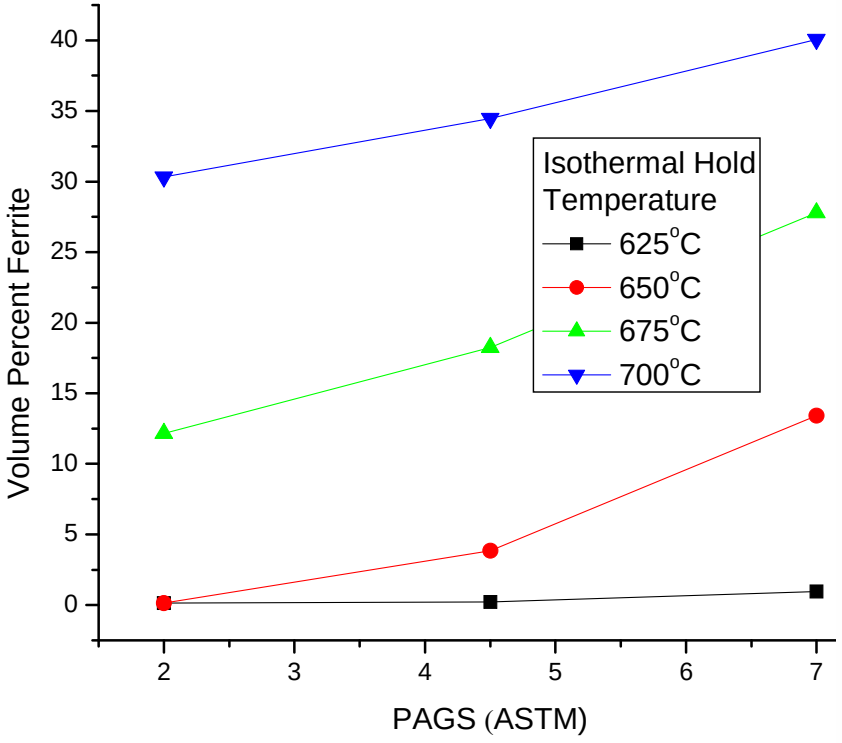

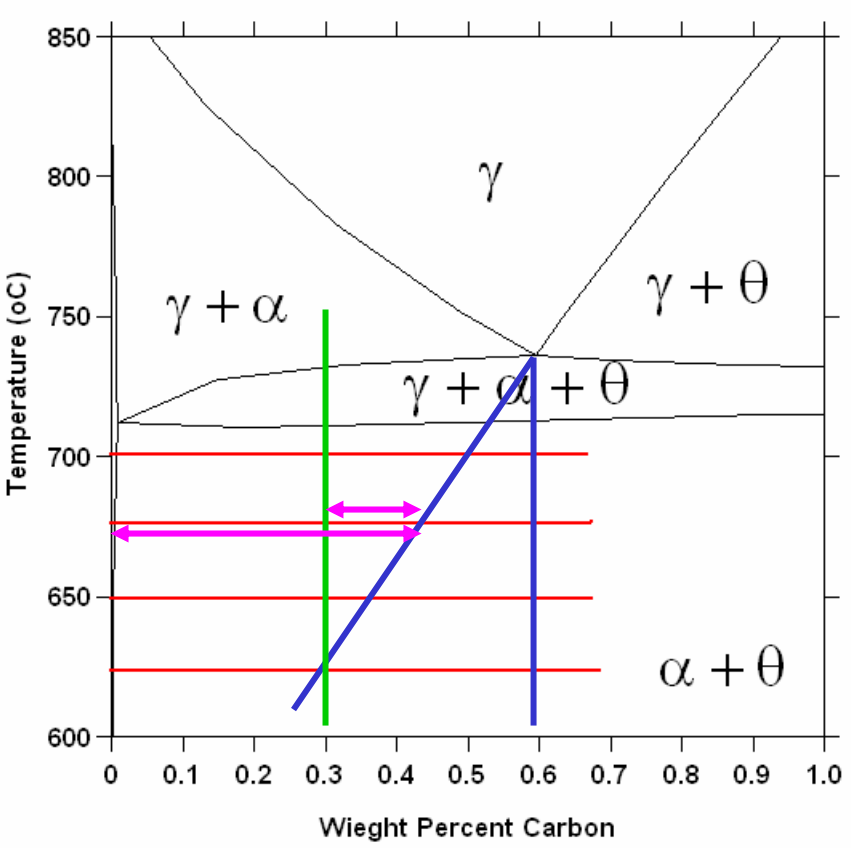

Advanced Steel Processing and Products Research Center

TIMKEN

1040 Steel – 670˚C Isothermal Hold

10 μm, 60% F, 40% P

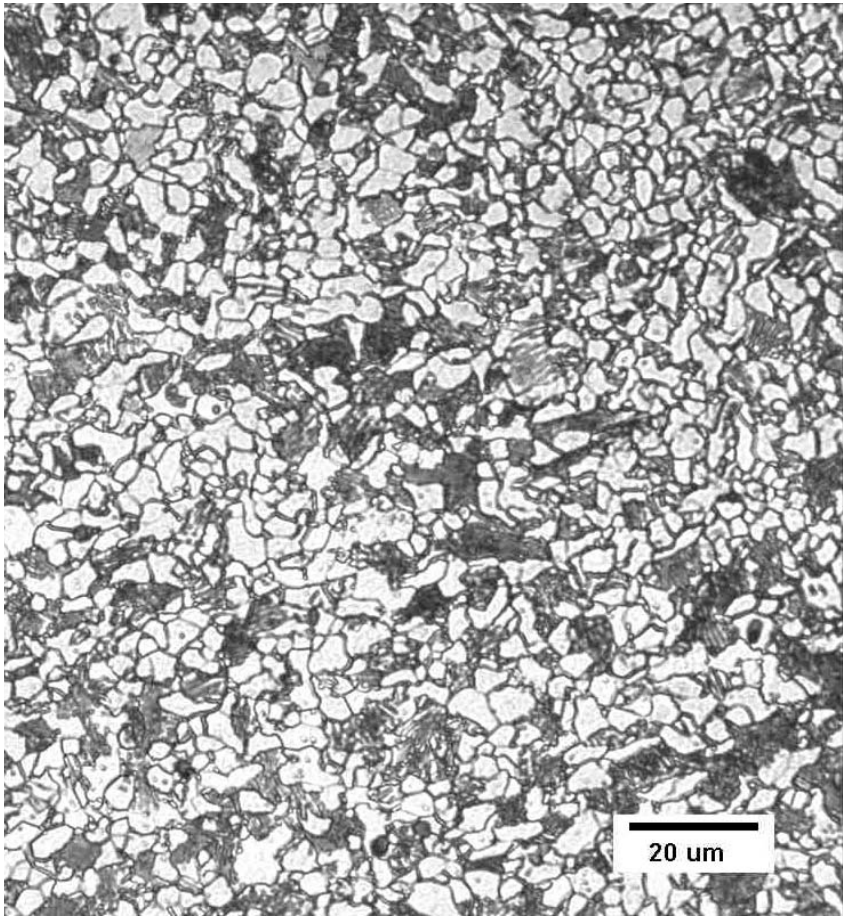

250 μm, 24% F, 76% P

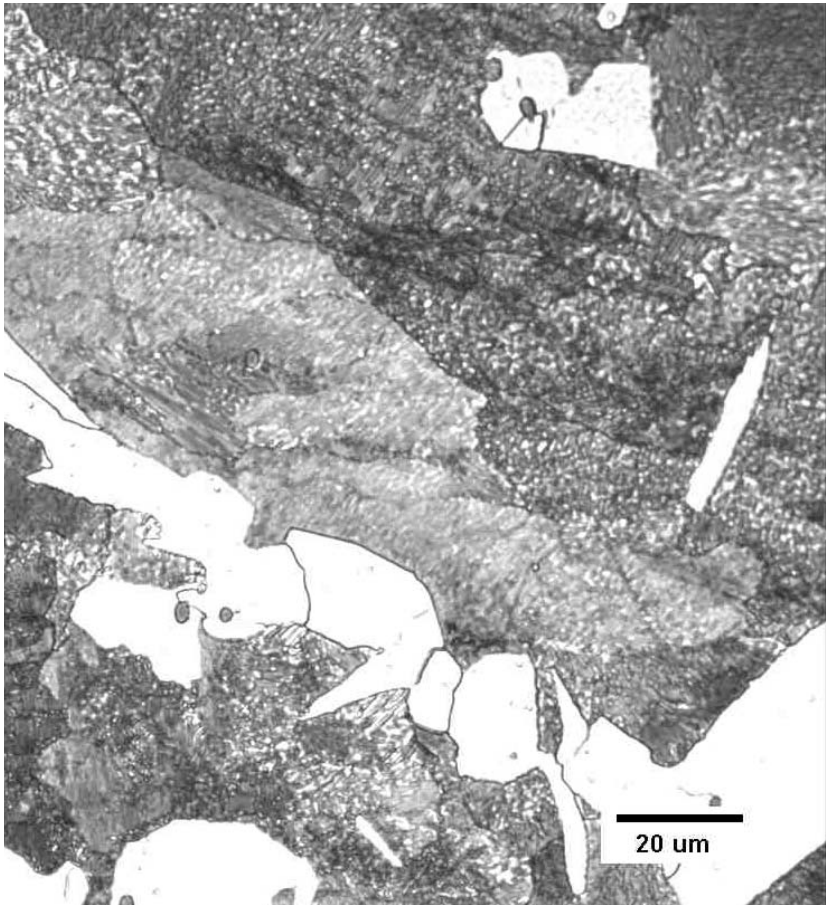

- Coarser prior austenite grain exhibits thicker ferrite half thickness

Advanced Steel Processing and Products Research Center

Relevance

Industrial Relevance

- Microstructures lead to properties
- Prior Austenite Grain Size…
  - Can be manipulated via heat treatment (i.e. normalizing)
  - Can be controlled with thermomechanical processing and/or microalloying
  - Is often left uncontrolled (i.e. forging, or tube & bar rolling)

Scientific Relevance

- Despite decades of ferrite growth research, we continue to lack a quantitatively accurate, physically based description for ferrite growth. This work sheds new light on aspects that must be incorporated.

TIMKEN

Thesis Questions and Outline

This work asks the following questions;

1. How does prior austenite grain size affect ferrite growth rate and final ferrite (1/2) thickness in ferrite + pearlite microstructures?
2. What is the effect of grain size on the establishment of conditions for pearlite nucleation and growth?

In order to address these questions the following tasks were pursued.

1. Generation of simple binary and ternary alloys for laboratory investigation,
2. Evaluation and observations of the ferrite growth rate and final ferrite (1/2) thickness using a range of experimental techniques, and
3. Application or generation of physically based mesoscale analytical models that predict the above experimental observations.

TIMKEN

Experimental Alloy Preparation

Alloy	C	Mn	Cr	Al	O(ppm)	N(ppm)
Fe-0.1C	0.14	0.01	0.01	0.009	78	8
Fe-0.3C	0.33	0.01	0.01	0.002	28	8
Fe-0.3C-1.0Mn	0.33	0.94	0.01	0.003	36	7
Fe-0.3C-3.0Mn	0.34	2.93	0.01	0.004	30	8
Fe-0.3C-3.0Cr	0.34	0.01	3.03	0.006	27	7
Nominal Others - Si, Ni, Mo, Cu, S = 0.01; Sn, V, Ti = 0.001, Co, P, W = 0.002						

- 45 kg Vacuum Induction Melted heats
- Electrolytic iron feed
- Killed with carbon (to avoid Al, Si)
- Forged and rolled ~ 90% R.A.
- Ternaries homogenized at 1200^{o}C – 36 hours

Fe-0.1C – Transforms too fast and with too much ferrite

Fe-0.3C-3X – Transforms too slow and with nil ferrite

TIMKEN

Dilatometry Samples

Max cooling rate

10˚C/s

70˚C/s

300˚C/s

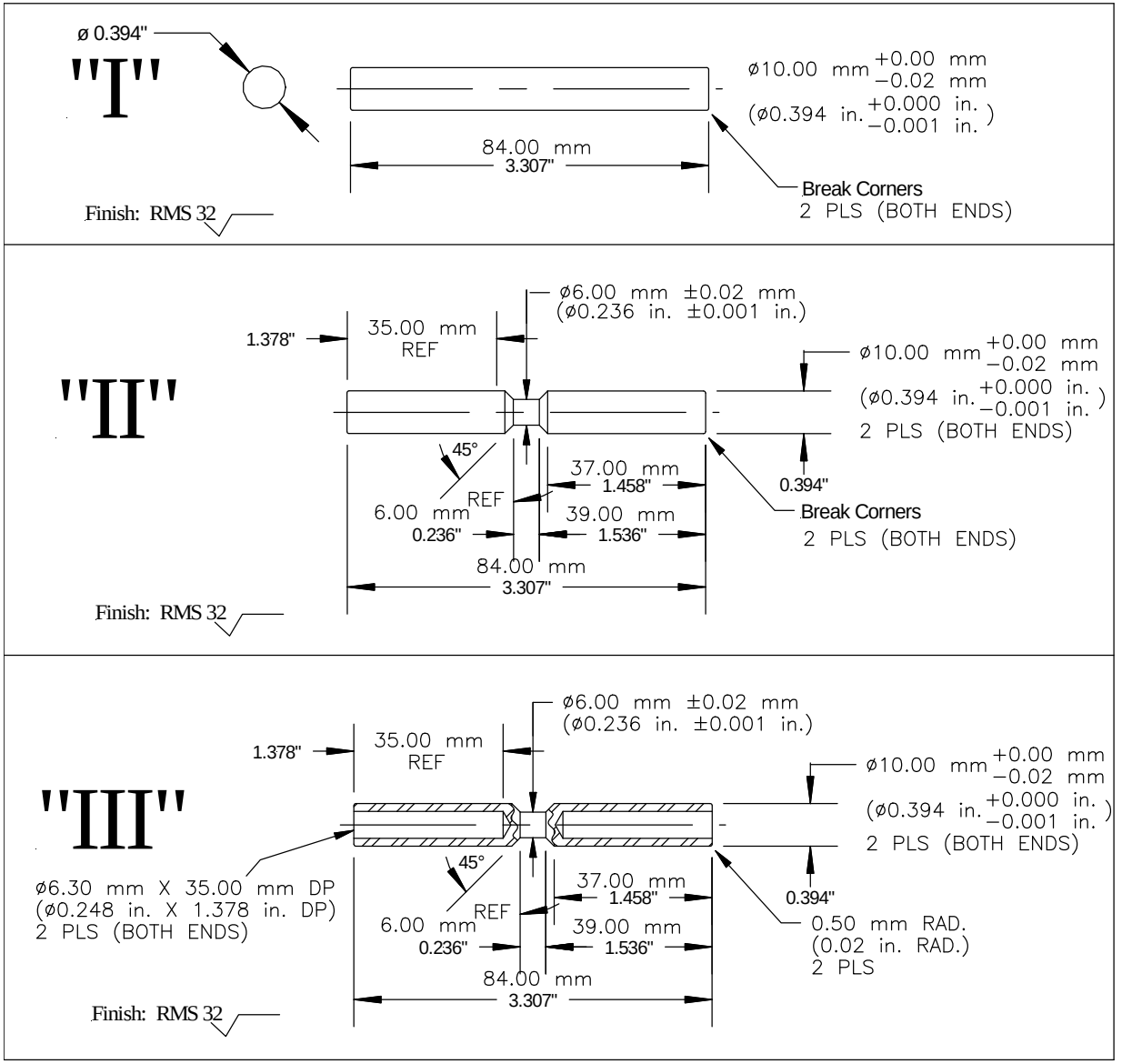

Advanced Steel Processing and Products Research Center

TIMKEN

Thermal Cycles

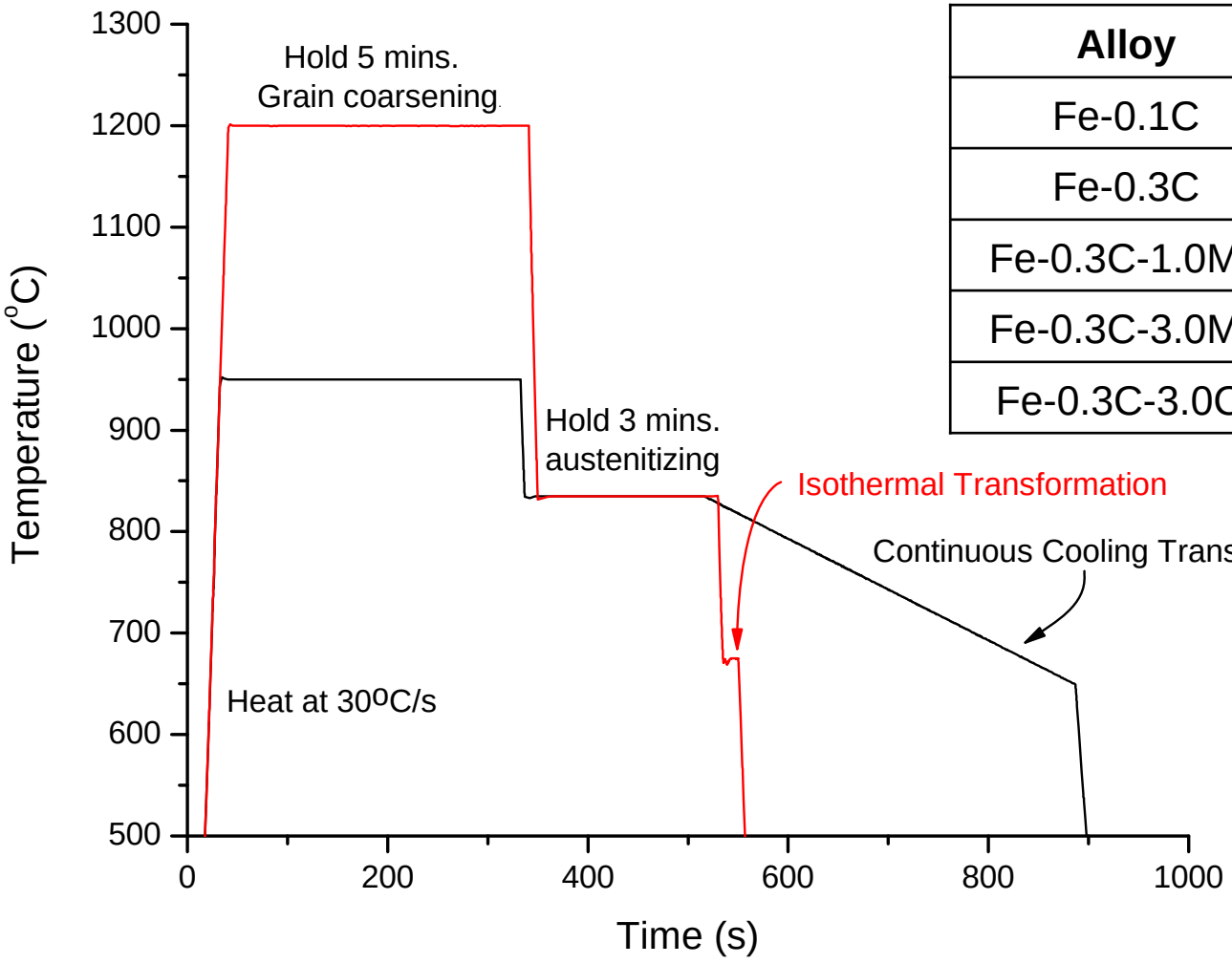

Austenitizing Temperature

Alloy	T_γ
Fe-0.1C	900
Fe-0.3C	835
Fe-0.3C-1.0Mn	815
Fe-0.3C-3.0Mn	770
Fe-0.3C-3.0Cr	825

Advanced Steel Processing and Products Research Center

TIMKEN

Results and Discussion

Microstructural Evolution

Modeling Vs. Experiment

Advanced Steel Processing and Products Research Center

TIMKEN

Grain Size Establishment

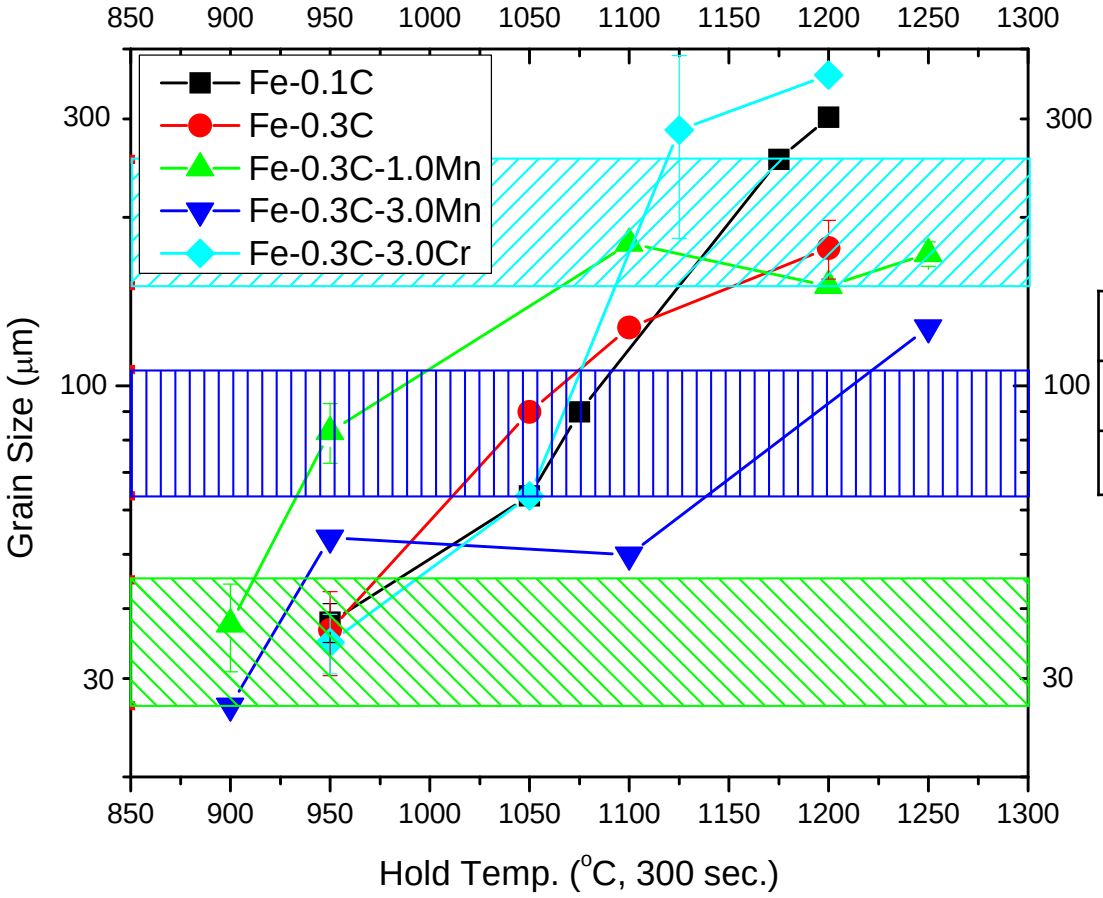

Nominal PAGS Diameters

'Fine'	ASTM 6.5	35-40 μm
'Medium'	ASTM 4	85-90 μm
'Coarse'	ASTM 2	170-180 μm

Solute drag Vs. Grain boundary energy/mobility?

Advanced Steel Processing and Products Research Center

TIMKEN

Fe-0.3C, PAGS Vs. ϕ_α

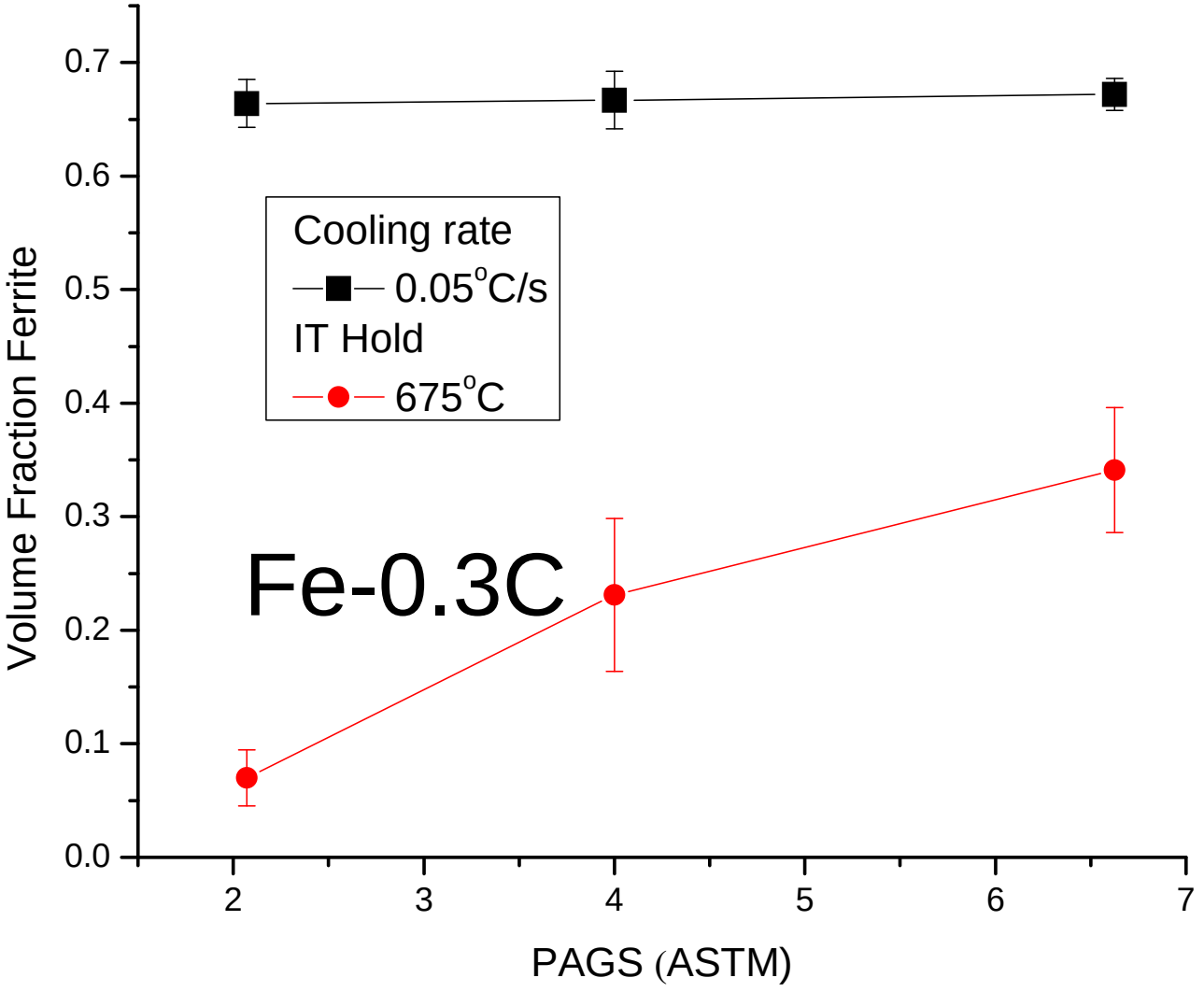

Advanced Steel Processing and Products Research Center

TIMKEN

Fe-0.3C-1.0Mn, PAGS Vs. ϕ_α

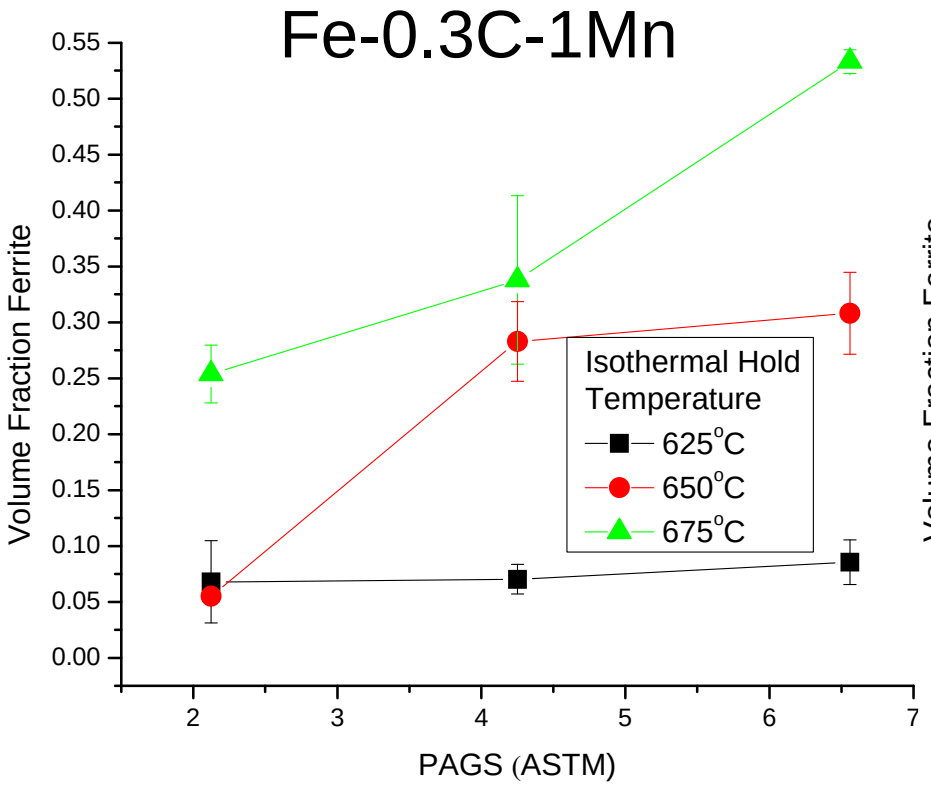

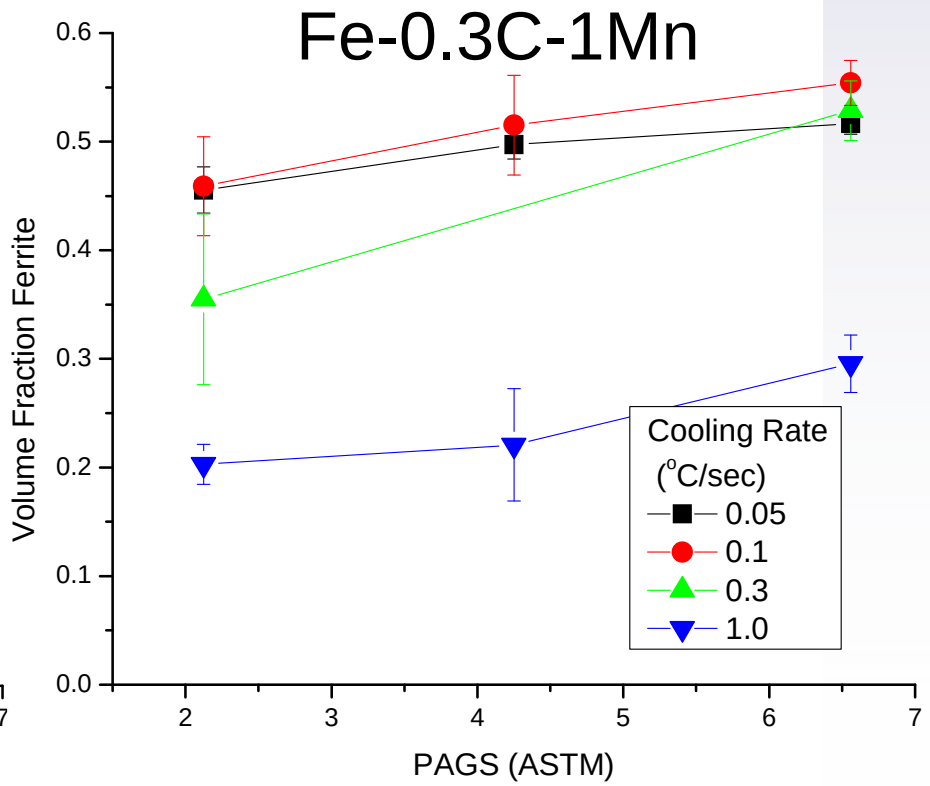

Advanced Steel Processing and Products Research Center

TIMKEN

Fe-0.3C-1.0Mn, CCT at 0.1˚C/s

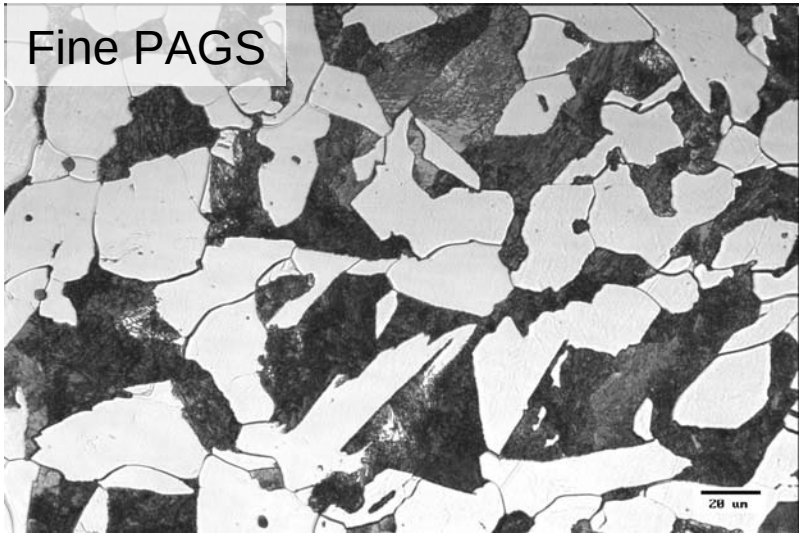

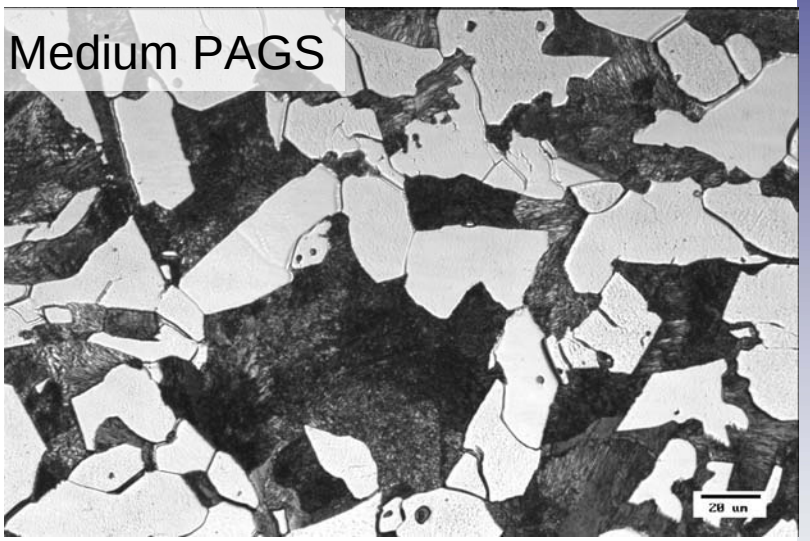

Fe-0.3C-1.0Mn

CCT Trends

- PAGS ↑, ϕ_α ↓
- PAGS ↑, $t_{1/2}$ ↑

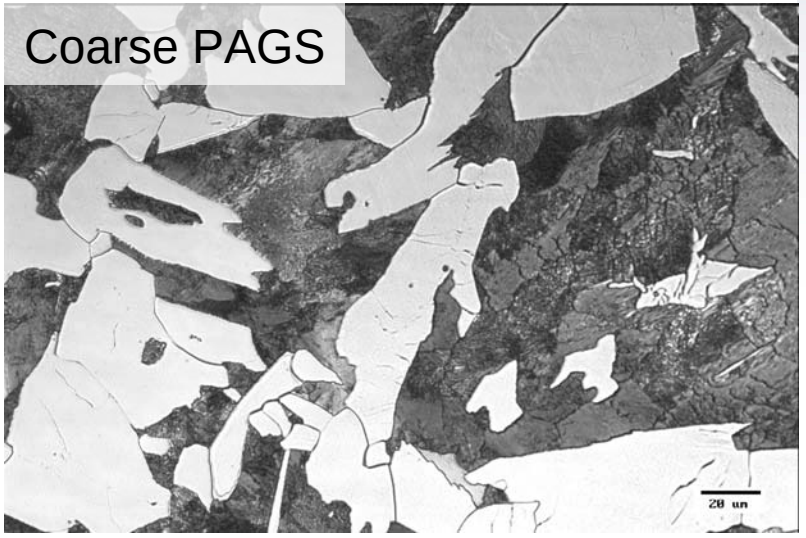

Advanced Steel Processing and Products Research Center

Fe-0.3C-1.0Mn, IT at 675˚C

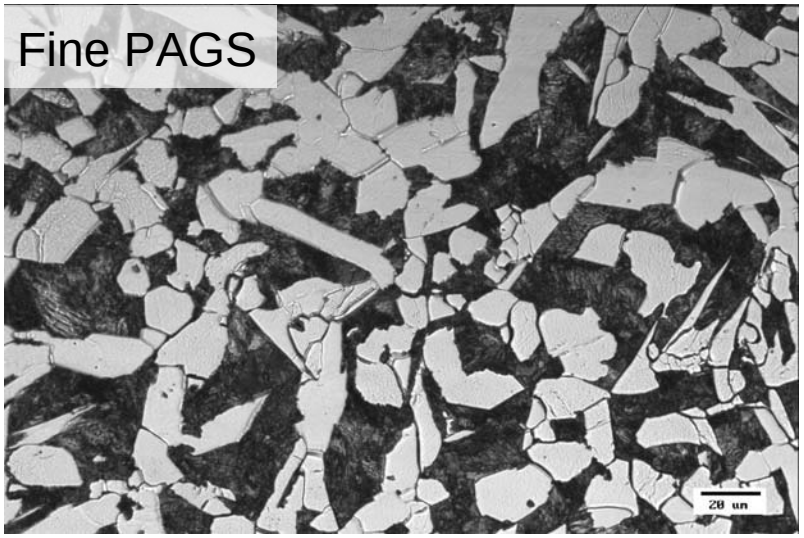

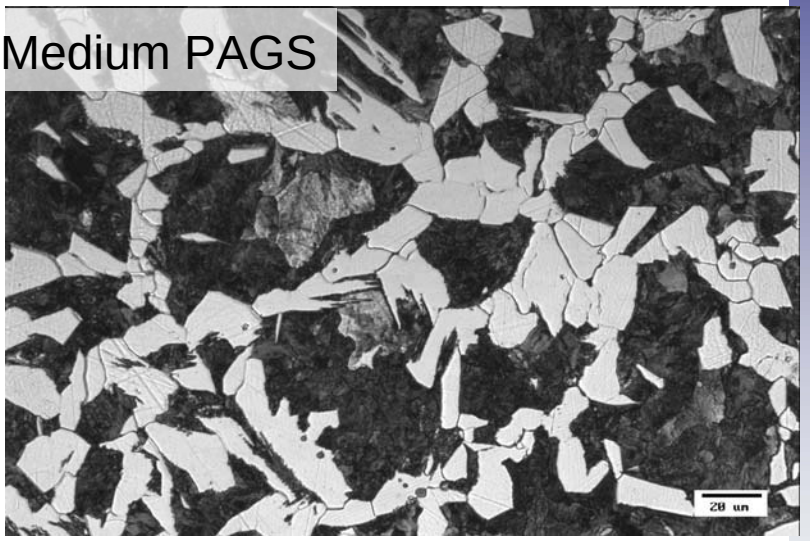

Fe-0.3C-1.0Mn

IT Trends

- PAGS ↑, ϕ_α ↓
- PAGS ↑, $t_{1/2}$ ↑

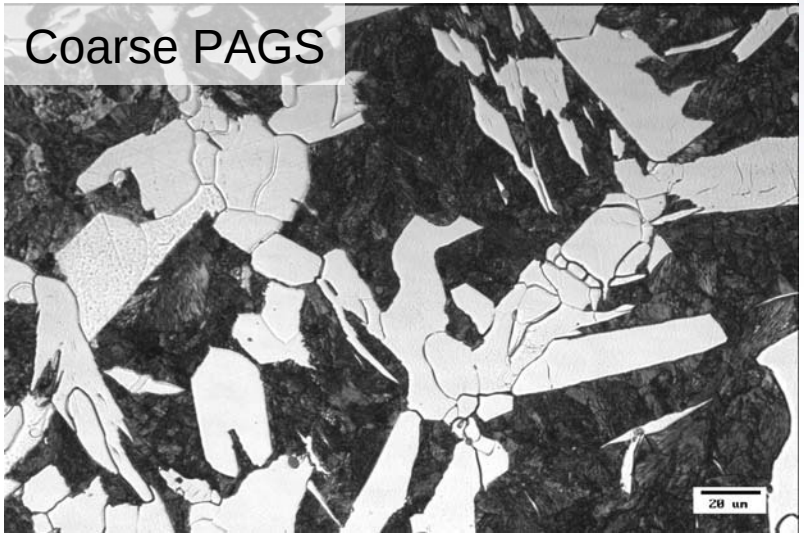

TIMKEN

Transformation Reaction Path

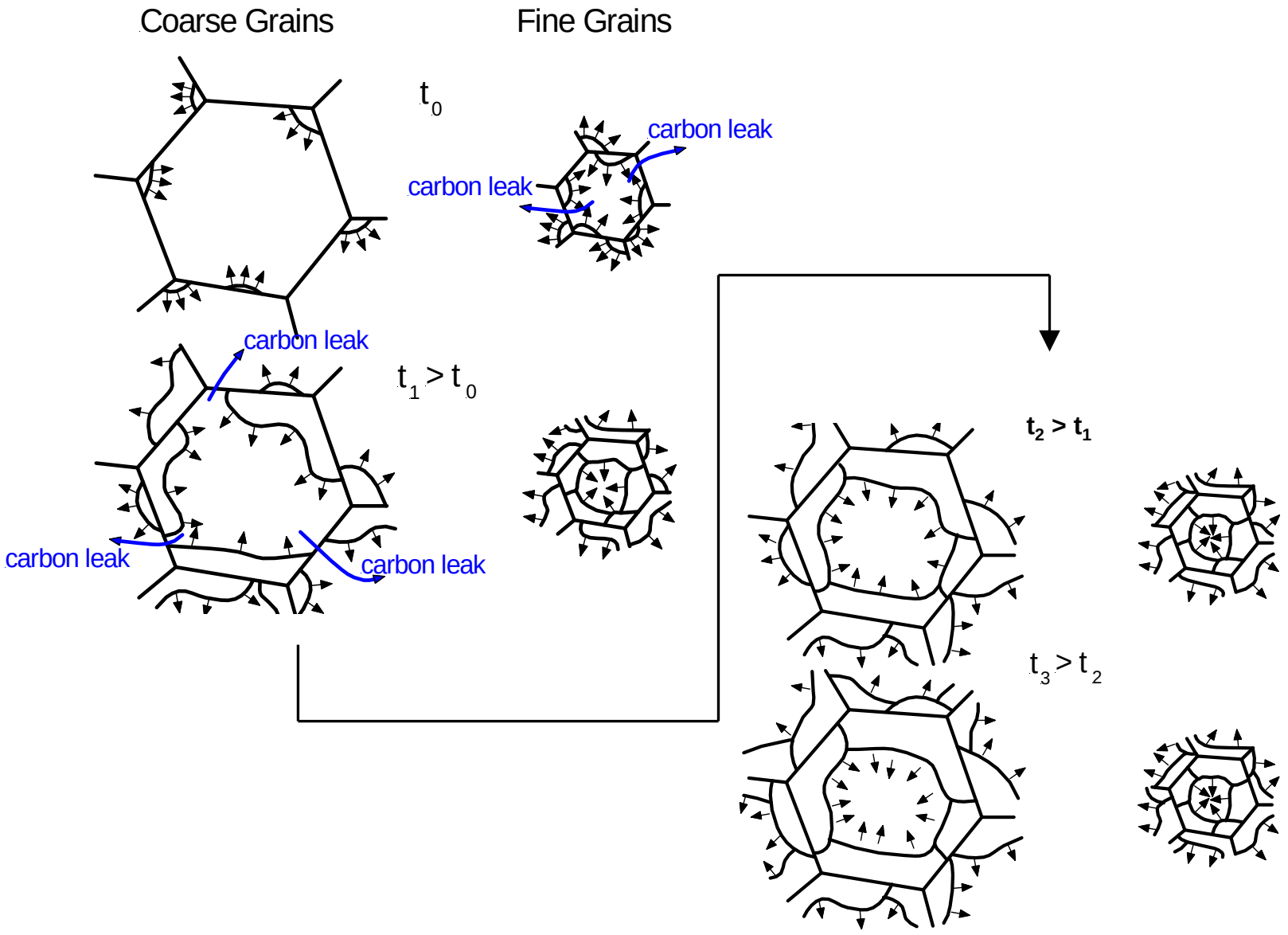

Advanced Steel Processing and Products Research Center

TIMKEN

Fe-0.3C, Planar Vs. Spherical IT Growth

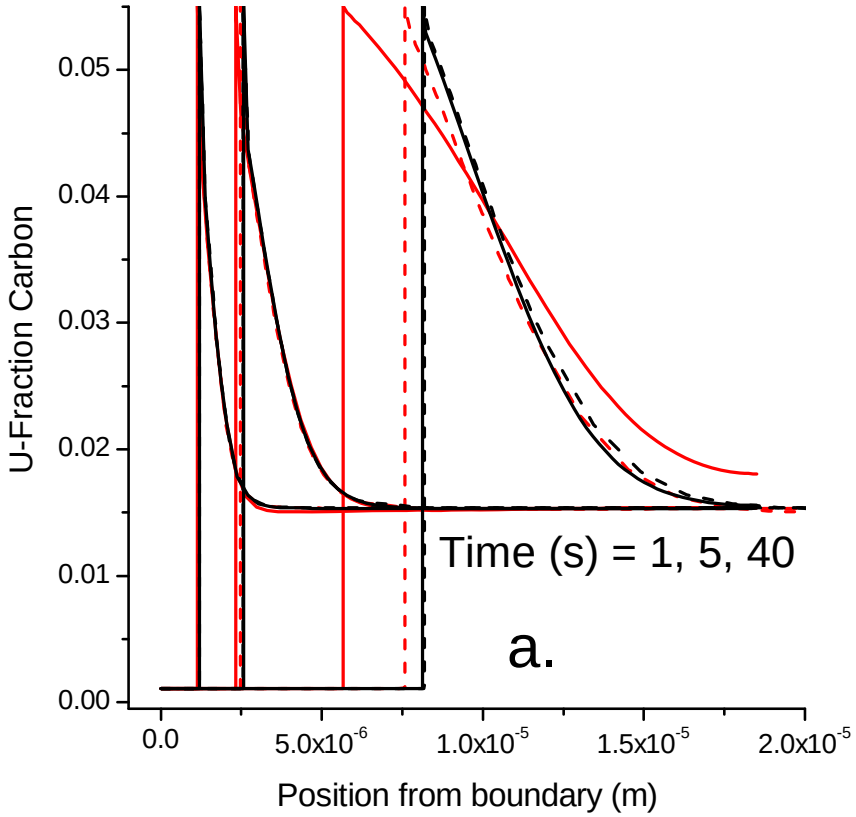

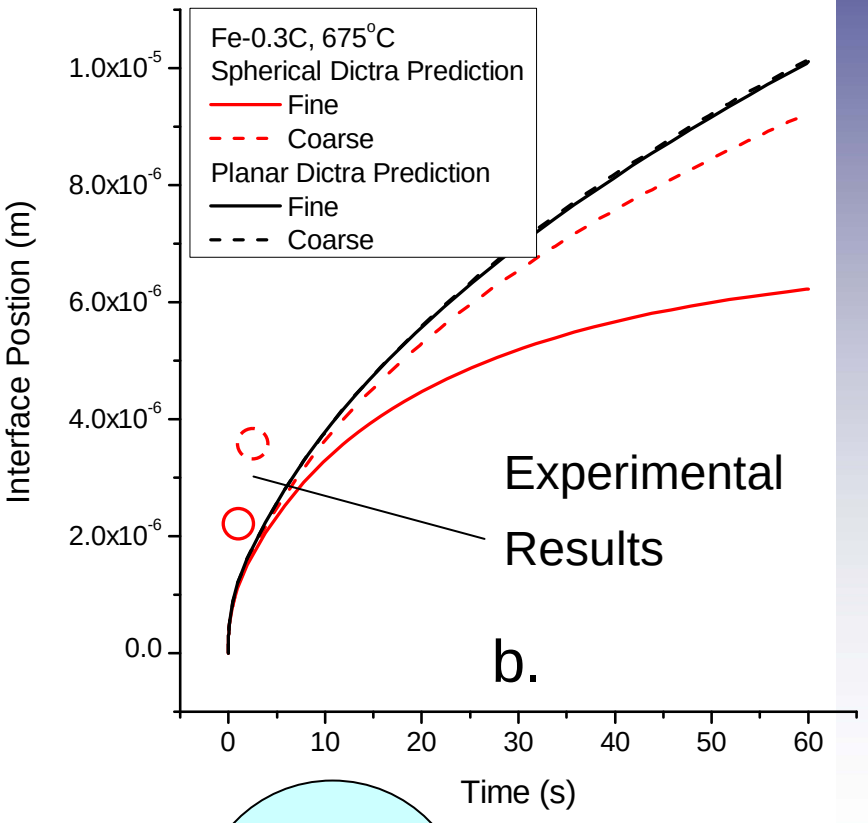

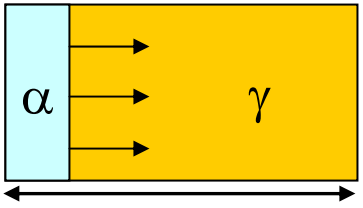

planar

½ PAGS

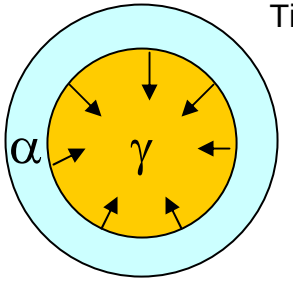

Spherical

PAGS

Advanced Steel Processing and Products Research Center

TIMKEN

Fe-0.3C-1.0Mn, Planar Vs. Spherical IT Growth

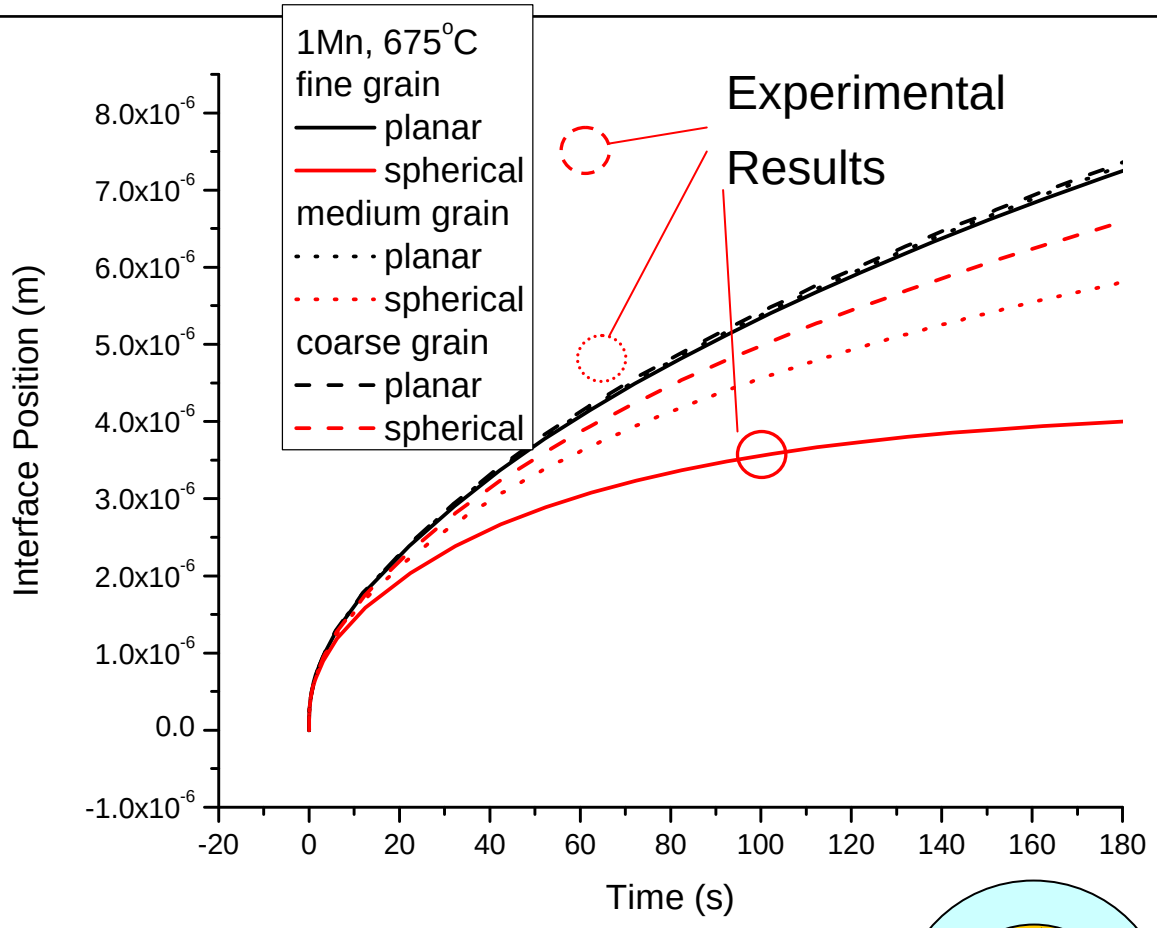

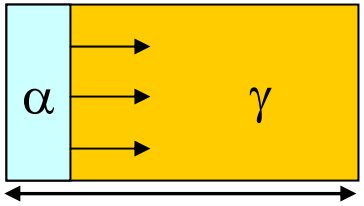

planar

½ PAGS

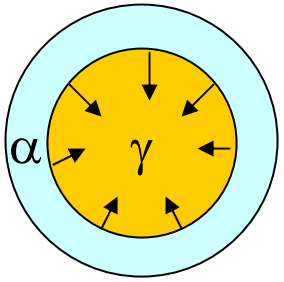

Spherical

PAGS

Advanced Steel Processing and Products Research Center

TIMKEN

Fe-0.3C, Planar Vs. Spherical CCT Growth

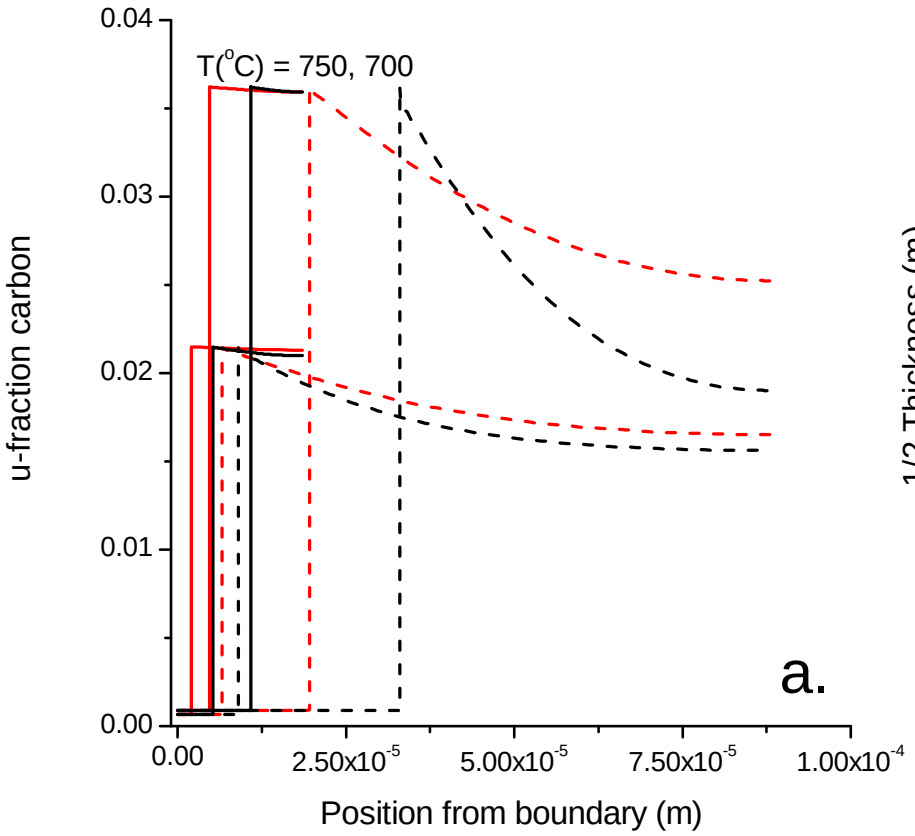

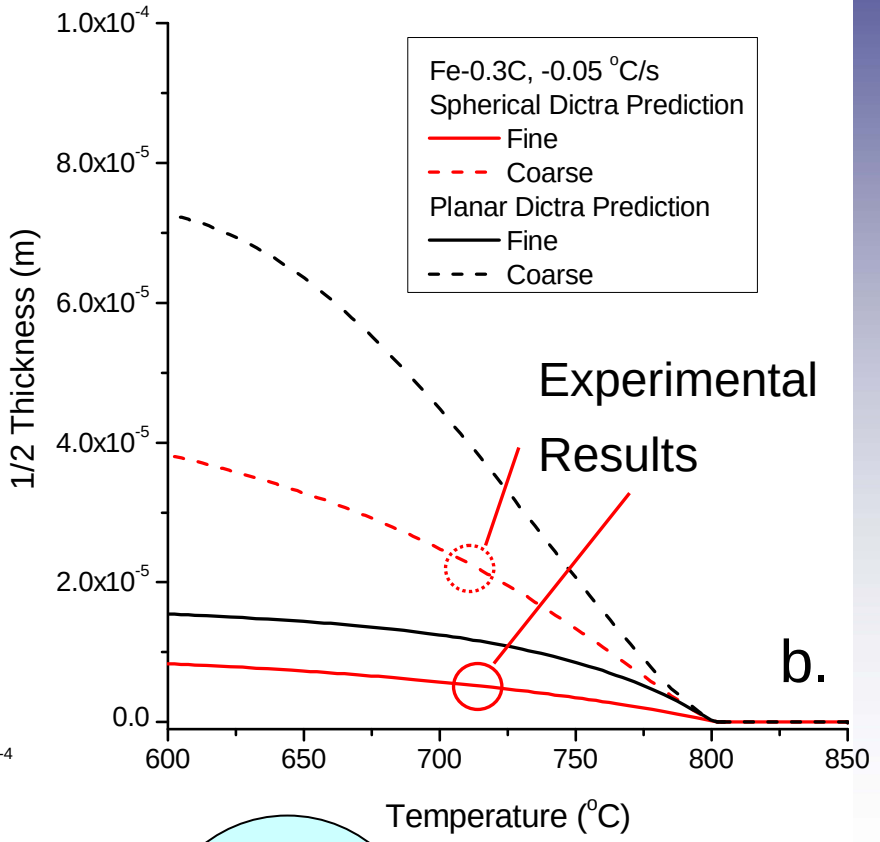

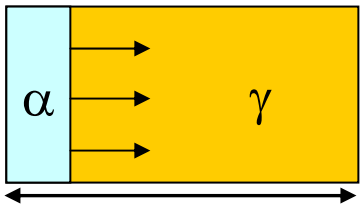

planar

½ PAGS

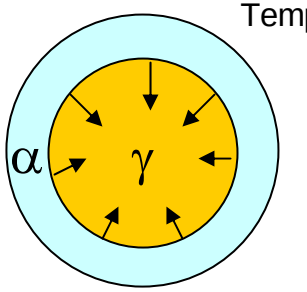

Spherical

PAGS

Advanced Steel Processing and Products Research Center

What Has Been Established?

- PAGS impacts the volume of austenite available to accept carbon.
- A small volume of austenite reduces the steepness of the carbon profile and diminishes the driving force.
- At sufficiently small grain sizes and with certain IT or CCT conditions, soft impingement can further impact ferrite growth rate.
- Diffusion Control Mode (DCM) simulations often under predict the ferrite $t_{1/2}^{\alpha}$ when compared to experiment.

What is Next? –

Comparing Experimental Growth Rate to

Modeled Growth Rate

Dilatometry Data Conversion

Provides volume fraction (ϕ_i) at each time and temperature from dilation data

Lattice parameters

- $a_\gamma = F[T, C]$
- $a_\alpha = F[T]$
- $a_{Fe_3C}, b_{Fe_3C}, c_{Fe_3C} = F[T]$
- $a_m, c_m = F[T, C]$

Carbon

- During ferrite formation austenite is enriched
- Pearlite, bainite and martensite are treated as neutral (i.e. the carbon in austenite after ferrite stops defines the carbon/cementite in the next phase/constituent)
- Superior approach compared to the 'lever rule'

Interface Position and Velocity

Approach

- Convert dilation data to ferrite phase fraction based on temperature, carbon and phase dependant lattice parameters
- Convert ferrite phase fraction data to interface position and velocity assuming spherical grains

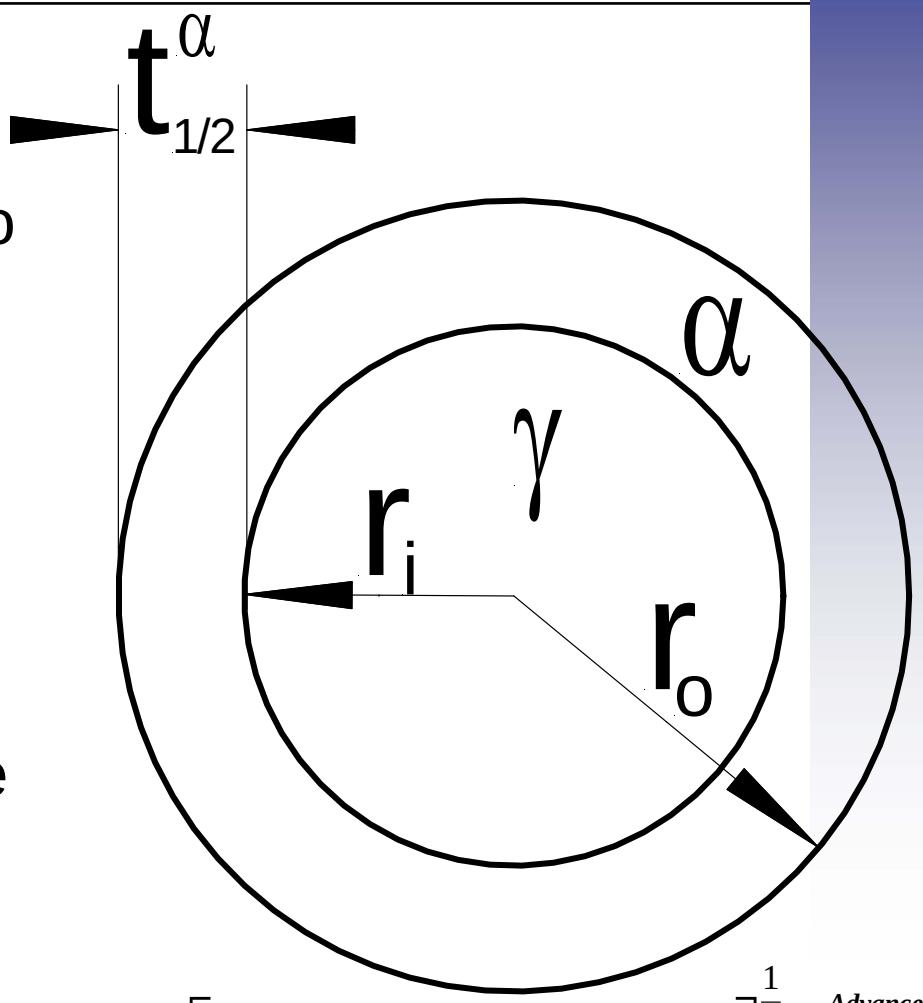

$$t_{1/2}^{\alpha} = r_0 - \left[\frac{3}{4\pi} \left(V_{PAGS_0} - V_f^{\alpha} V_{PAGS_0} \right) \right]^{\frac{1}{3}}$$

Fe-0.3C, DCM Vs. Experiment

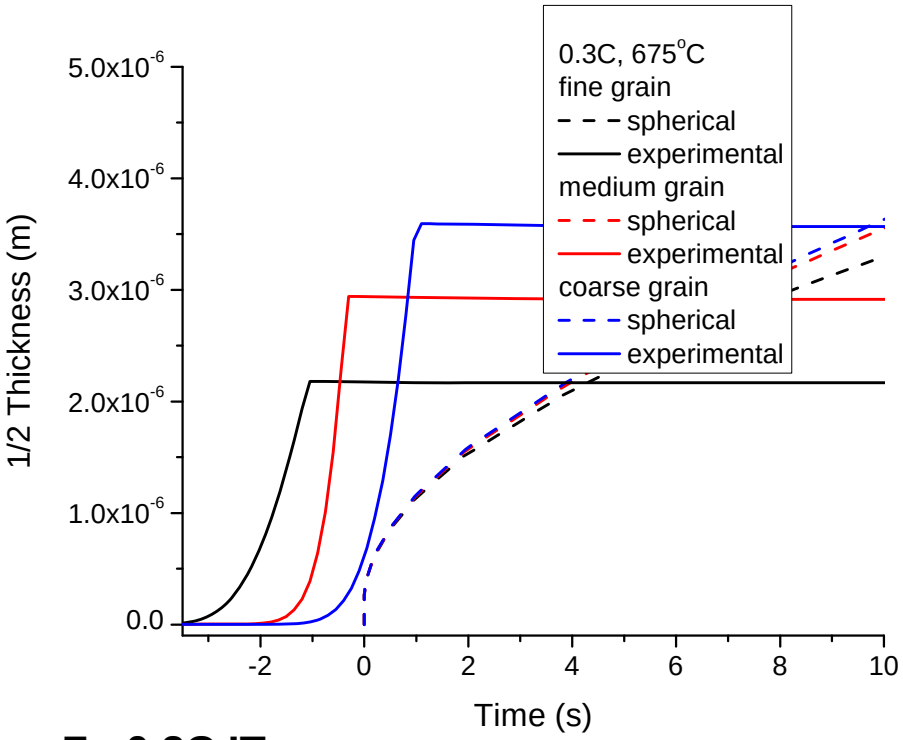

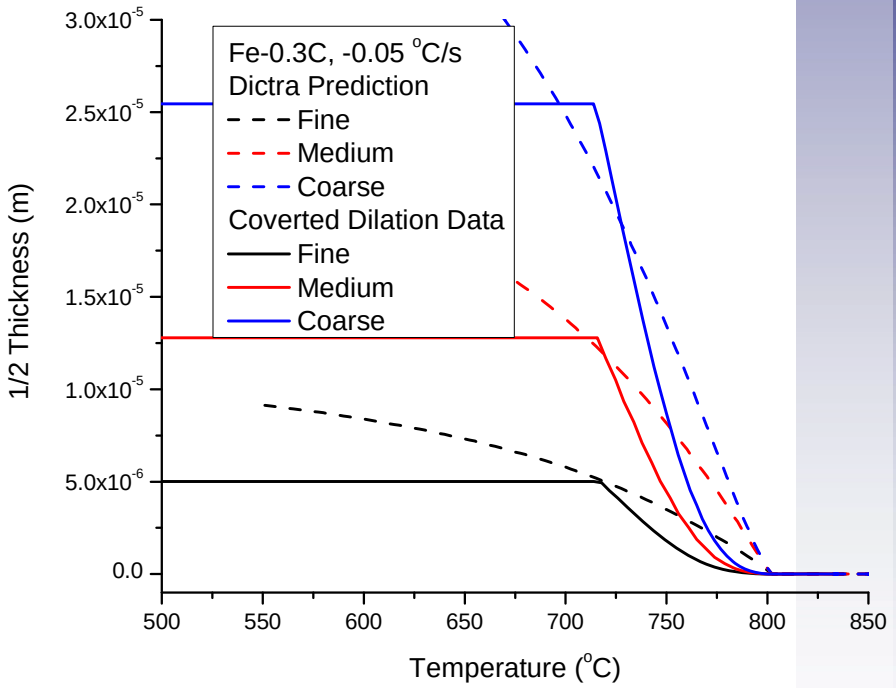

Fe-0.3C IT summary

At 700°C, Widmenstätten ferrite formed for coarse grains

At 650°C, Hardenability problems exacerbated

Fe-0.3C CCT summary

When Widmenstätten was not present, DCM simulations provided reasonable final ferrite 1/2 thickness

For both IT and CCT, DCM over predicted early and under predicted later growth rate.

Advanced Steel Processing and Products Research Center

TIMKEN

Fe-0.3C Experimental Vs. DCM Ferrite $t^{\alpha}_{1/2}$

Isothermal Hold (°C)	Fine Grain		Medium Grain		Coarse Grain	
	Sim.	Exp.	Sim.	Exp.	Sim.	Exp
700	2.7	5.3	N-R	N-R	Wid.	Wid.
675	Unk.	2.2	Unk.	2.9	1.2	3.6
650	Unk.	1.0	Unk.	1.0	Unk.	1.3

Cooling Rate (°C/s)	Fine Grain		Medium Grain		Coarse Grain	
	Sim.	Exp.	Sim.	Exp.	Sim.	Exp.
0.05	5.0	5.0	N-R	N-R	22.2	25
0.1	N-R	N-R	12.3	12.8	Wid.	Wid.
0.5	5.1	4.7	9.4	10.4	N-R	N-R
1	5.2	4.2	7.8	8.0	N-R	N-R

Values in μm, N-R = Not Run, Wid. = Widmenstätten, Unk. = Unknown

Fe-0.3C-1.0Mn, DCM Vs. Experiment

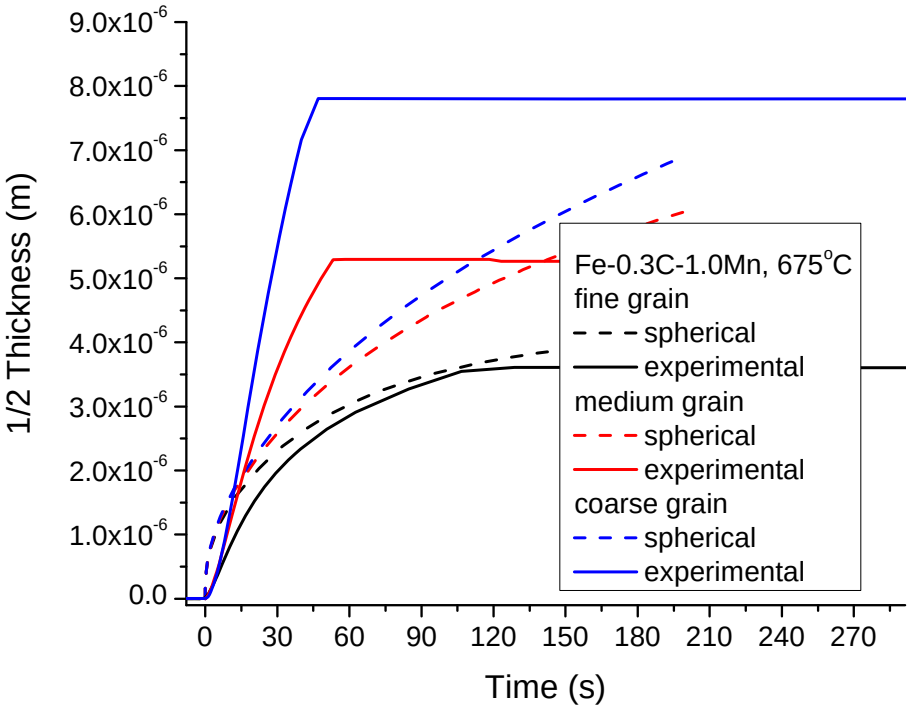

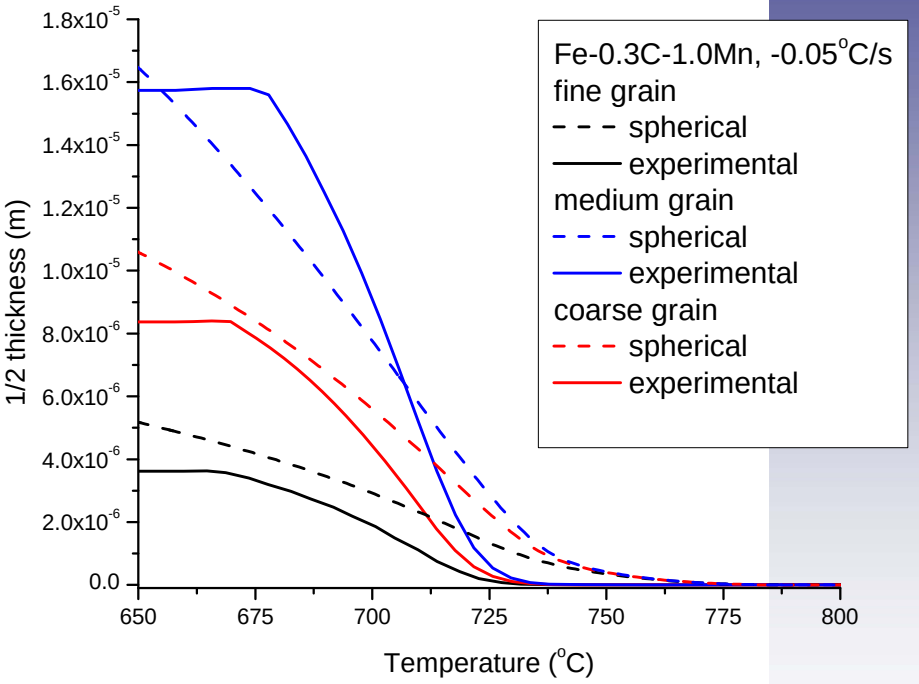

Fe-0.3C-1.0Mn IT Summary

Fine grains resulted in closer predictions while medium and coarse grains were again under predicted.

Fe-0.3C-1.0Mn CCT Summary

DCM simulations were closest for fine grains and provided reasonable final ferrite 1/2 thickness

For both IT and CCT, DCM over predicted early and under predicted later growth rate.

Advanced Steel Processing and Products Research Center

TIMKEN

Fe-0.3C-1.0Mn Experimental Vs. DCM $t^{\alpha}_{1/2}$

Isothermal Hold (°C)	Fine Grain		Medium Grain		Coarse Grain	
	Sim.	Exp.	Sim.	Exp.	Sim.	Exp.
675	3.6	3.6	3.4	5.3	3.4	7.8
650	1.3	1.4	1.3	2.1	1.3	2.5
625	0.8	0.4	0.9	0.7	1	1.2

Cooling Rate (°C/s)	Fine Grain		Medium Grain		Coarse Grain	
	Sim.	Exp.	Sim.	Exp.	Sim.	Exp.
0.05	4.6	3.6	9.0	8.4	12.8	15.7
0.1	N-R	3.5	N-R	7.4	N-R	13.0
0.3	4.3	3.3	N-R	N-R	7.0	10.2
1	N-R	N-R	N-R	3.1	N-R	5.7

Values in μm, N-R = Not Run

Advanced Steel Processing and Products Research Center

TIMKEN

What Else Has Been Established?

DCM, the supposed upper bound in growth rate over predicts initial growth, but more importantly, under predicts later growth.

At all IT or CCT conditions studied, PAGS impacts growth rate, but only minimally at PAGS > 175μm.

At sufficiently small PAGS, and with certain alloy and transformation conditions, DCM is nearly accurate because of soft impingement. (i.e. when the driving force is nearly consumed).

What is Next? –

Modifying initial and later growth rate with the Phase Field Method

TIMKEN

Phase Field Method Governing Equations

Conserved Fields (composition)

$$\frac{\partial c(\mathbf{r},t)}{\partial t} = -\nabla \bullet \mathbf{J} \qquad \text{Cahn-Hilliard} \quad \mathbf{J} = -M\nabla\mu$$

$$\mu = \frac{\delta F_{cg}}{\delta c} = \frac{\delta F_{\text{chem}}}{\delta c} + \frac{\delta F_{\text{elast}}}{\delta c} + \frac{\delta F_{\text{inter}}}{\delta c} + \ldots$$

Non-Conserved Fields (phases)

$$\frac{\partial \eta(\mathbf{r},t)}{\partial t} = -L\frac{\delta F_{cg}}{\delta \eta(\mathbf{r},t)}$$

Cahn-Allen, or Time Dependant Ginzburg-Landau

My System

Composition, $c_1 = Fe, c_2 = C, c_3 = Mn \ldots$

Order Parameter, $\eta_1 = \gamma, \eta_2 = \alpha, \eta_3 = \theta, \eta_4 = ASTM \ldots$

Advanced Steel Processing and Products Research Center

TIMKEN

The Phase Field Method

- The derivation of the phase field equations is consistent with thermodynamic and kinetic principles, and incorporates the apparent interface moblility.
- The derivation results in coupled partial differential equations (PDE's).
- Coupling occurs due to thermodynamic stability as a functions of local chemistry for the non-conserved (phase) field, and the thermodynamic driving force for diffusion for the conserved (composition) field.
- Solve coupled PDE's for conserved and non-conserved field variables.
- Additional terms are often added to account for anisotropic interfacial energy, grain orientation, etc. allowing for realistic simulations of 3-D morphologies
- Phase Field Models are Computationally Expensive!

Phase Field Modeling Results

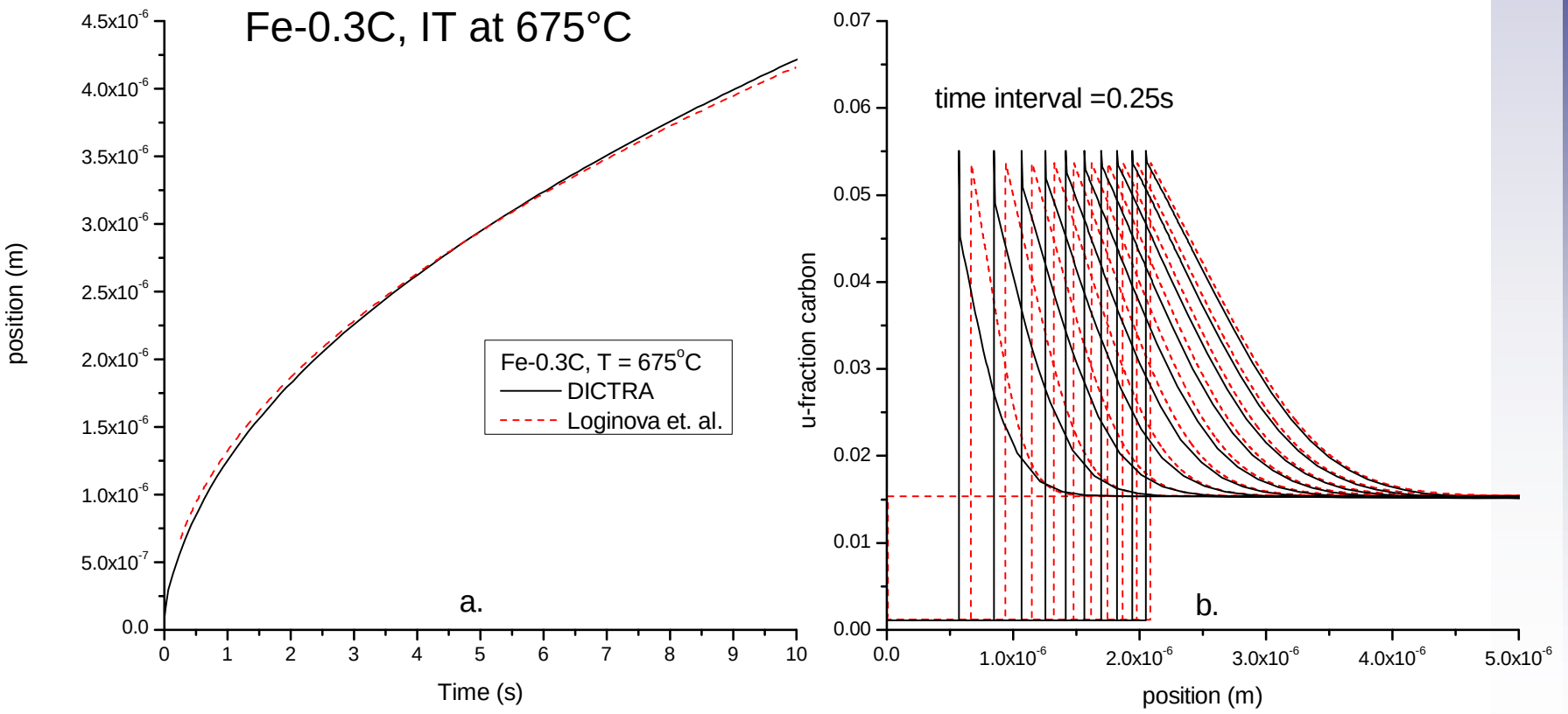

A phase field model was built based on the construct of Loginova et al. using FiPy (NIST general PDE tool), and the Loginova *et al.* 1-D test code was also obtained and used to run simulations.

As constructed these codes essentially give the same result as DICTRA.

TIMKEN

Apparent Phase Field Mobility

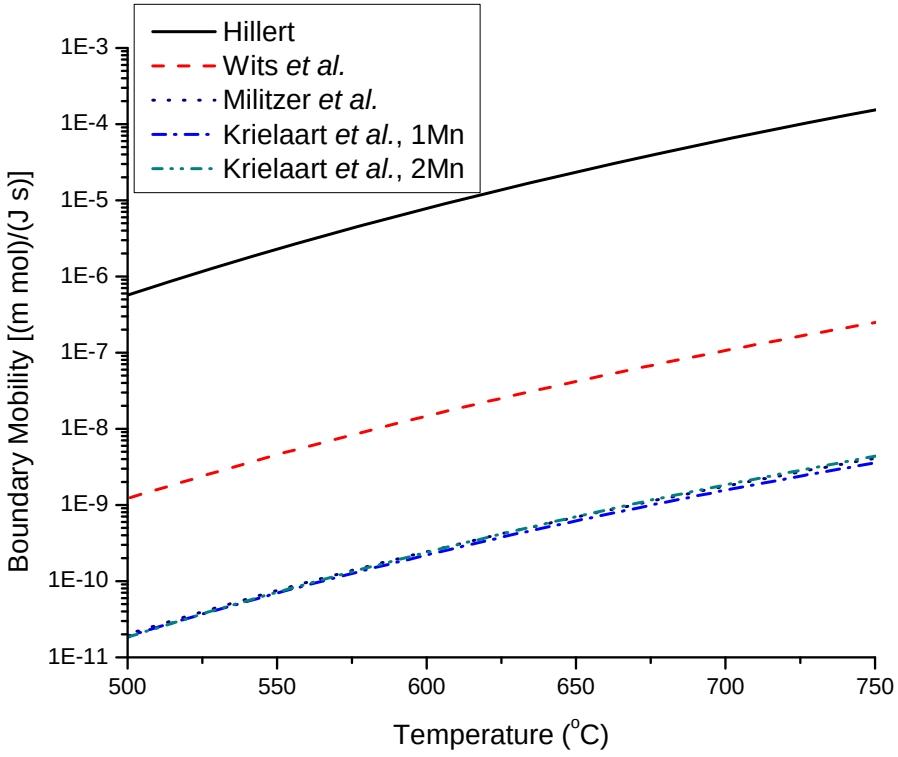

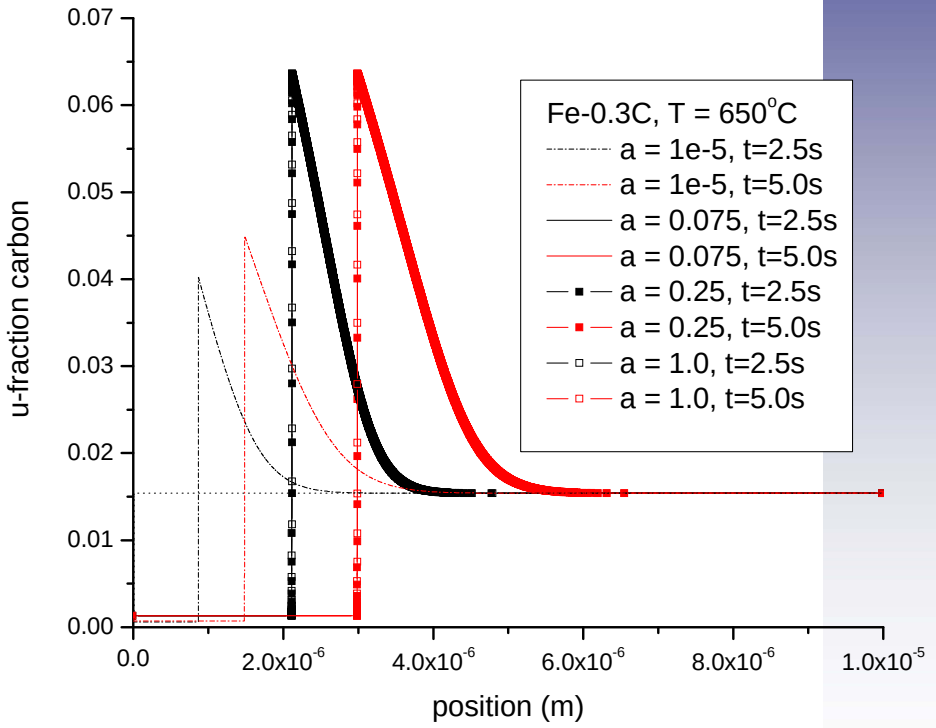

Hillert proposal based on α/α coarsening, others based on α growth in γ.

PFM results with $a*M_{Hillert}$ value show with the Hillert value the PFM reduces to DCM. Recent work by Hoagland et. Al. at KTH revised the Hillert Mobility down ~ 5 orders of magnitude

Advanced Steel Processing and Products Research Center

Diffusion of Carbon in Austenite

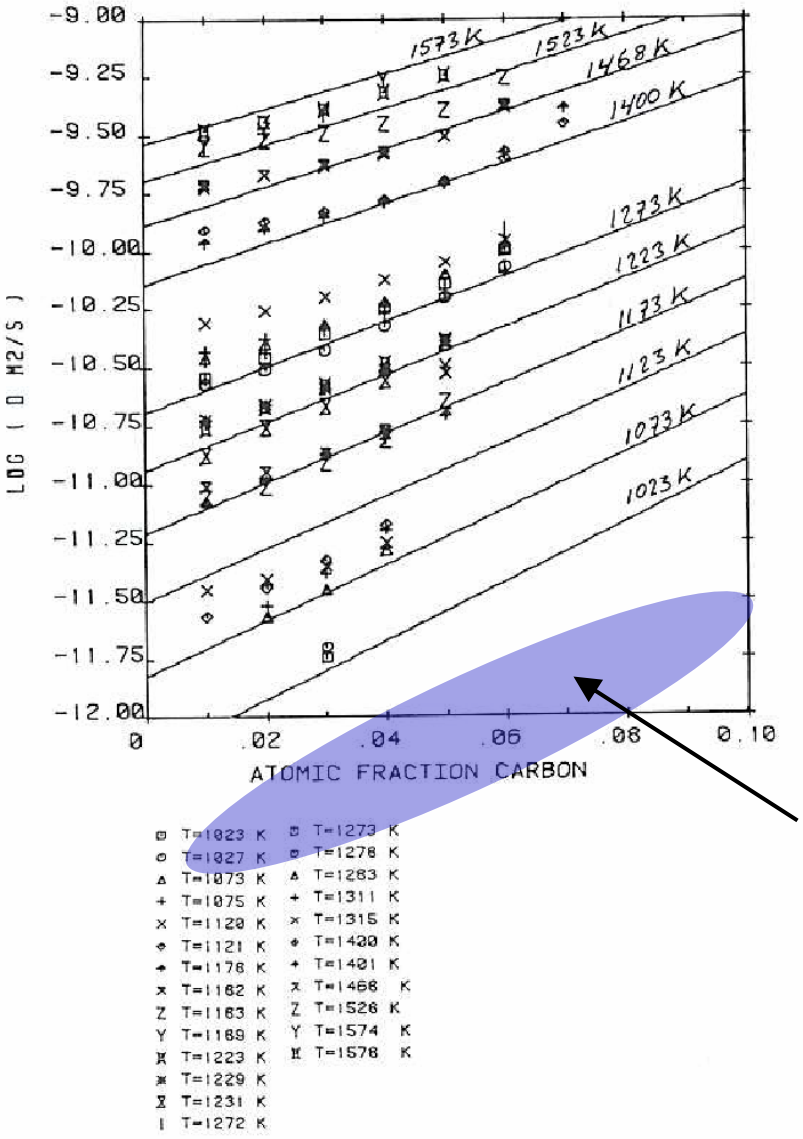

FIG. 1

The diffusion coefficient for carbon in γ-iron using atomic fraction as concentration variable. The symbols denote experimental values from Wells, Batz and Mehl (2), and the solid lines are calculated using the present analysis.

Current work is for temperatures of 625-725°C (900-1000°K) and carbon contents between 0.01 and 0.09 atomic fraction.

TIMKEN

PFM Results with Higher D_c^{γ}

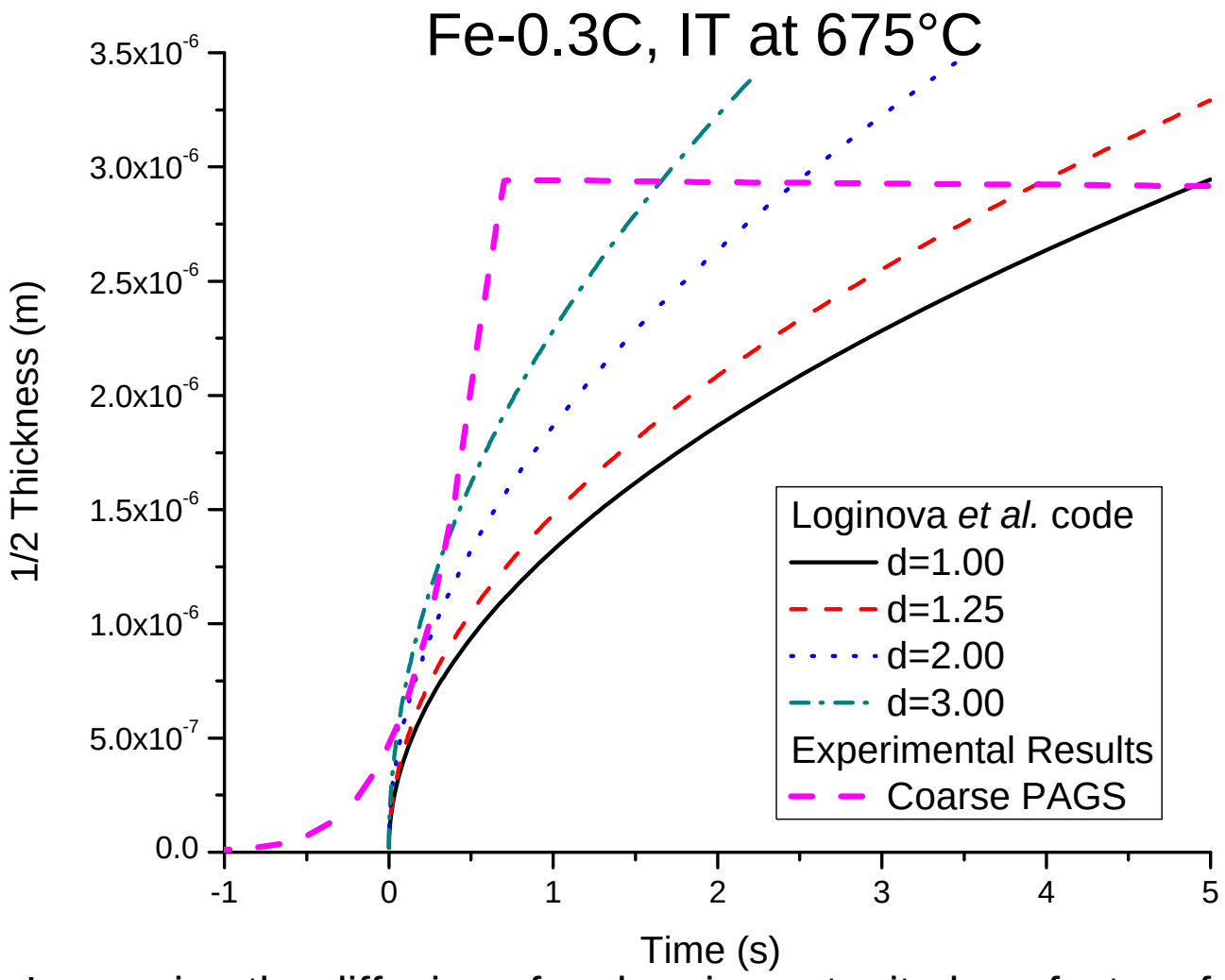

- Increasing the diffusion of carbon in austenite by a factor of ~ 3 or more in order to increase the rate of transformation to approximate the experimentally measured rate.

Advanced Steel Processing and Products Research Center

Conclusions

- For IT conditions the final ferrite ½ thickness decreases as the PAGS is reduced due to the reduced volume of austenite available to accept carbon.
- For CCT conditions the PAGS also impacts carbon accumulation, but for fine grains the occurrence of soft impingement and ‘filling’ reduces the strength of the PAGS on the final ferrite ½ thickness.
- Generally accepted D_c^{γ} functions under predict the carbon diffusivity in austenite at temperatures relevant to ferrite growth.
- DCM over predicts early ferrite growth and under predicts later ferrite growth.
- Phase Field Modeling can be used to allow early growth to proceed via ICM, and trend toward DCM as growth continues.

Future Work

- The current (each PAGS, IT & CCT, Fe-03C & Fe-0.3C-1.0Mn) results should be used in conjunction with spherical simulations and automated optimization techniques to arrive at more broadly acceptable apparent mobility and carbon diffusivity functions.
- PFM's should be further pursued in 3-D to generate a more detailed understanding of the nucleation, carbon leaking and transformation domain (PAGS) issues.
- Deep penetrating X-rays from a synchrotron source should continue to be exploited to understand how ferrite forms in 3-D space.

TIMKEN

Thank You!

Questions and Discussion

Advanced Steel Processing and Products Research Center

TIMKEN

Extra Slides

TIMKEN

Free Energy and Nucleation

Advanced Steel Processing and Products Research Center

TIMKEN

Carbon Profiles

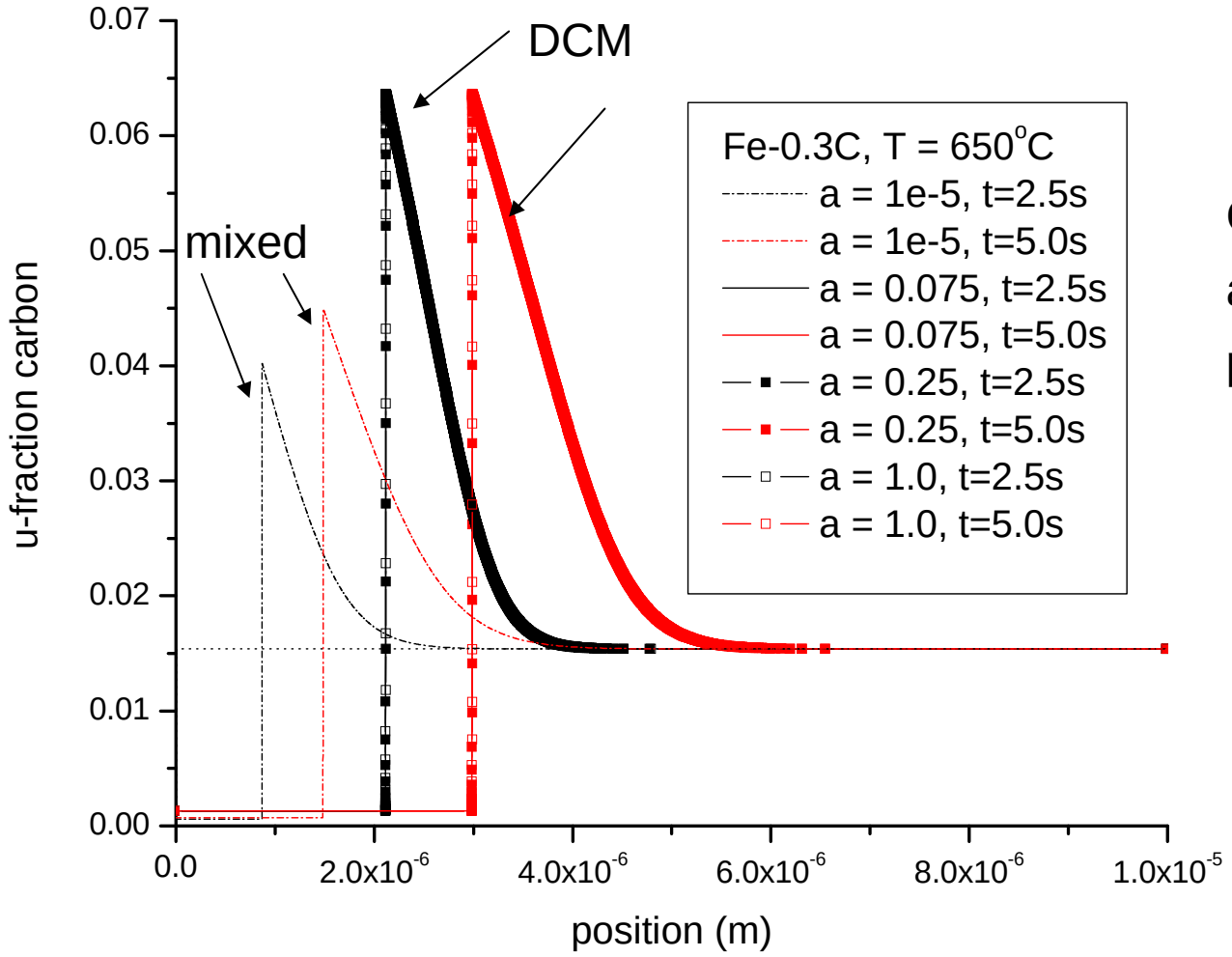

Carbon content at each point = C_i

Figure show profiles for DCM, and mixed DCM/ICM conditions

Advanced Steel Processing and Products Research Center

TIMKEN

Effect of Temperature on The System

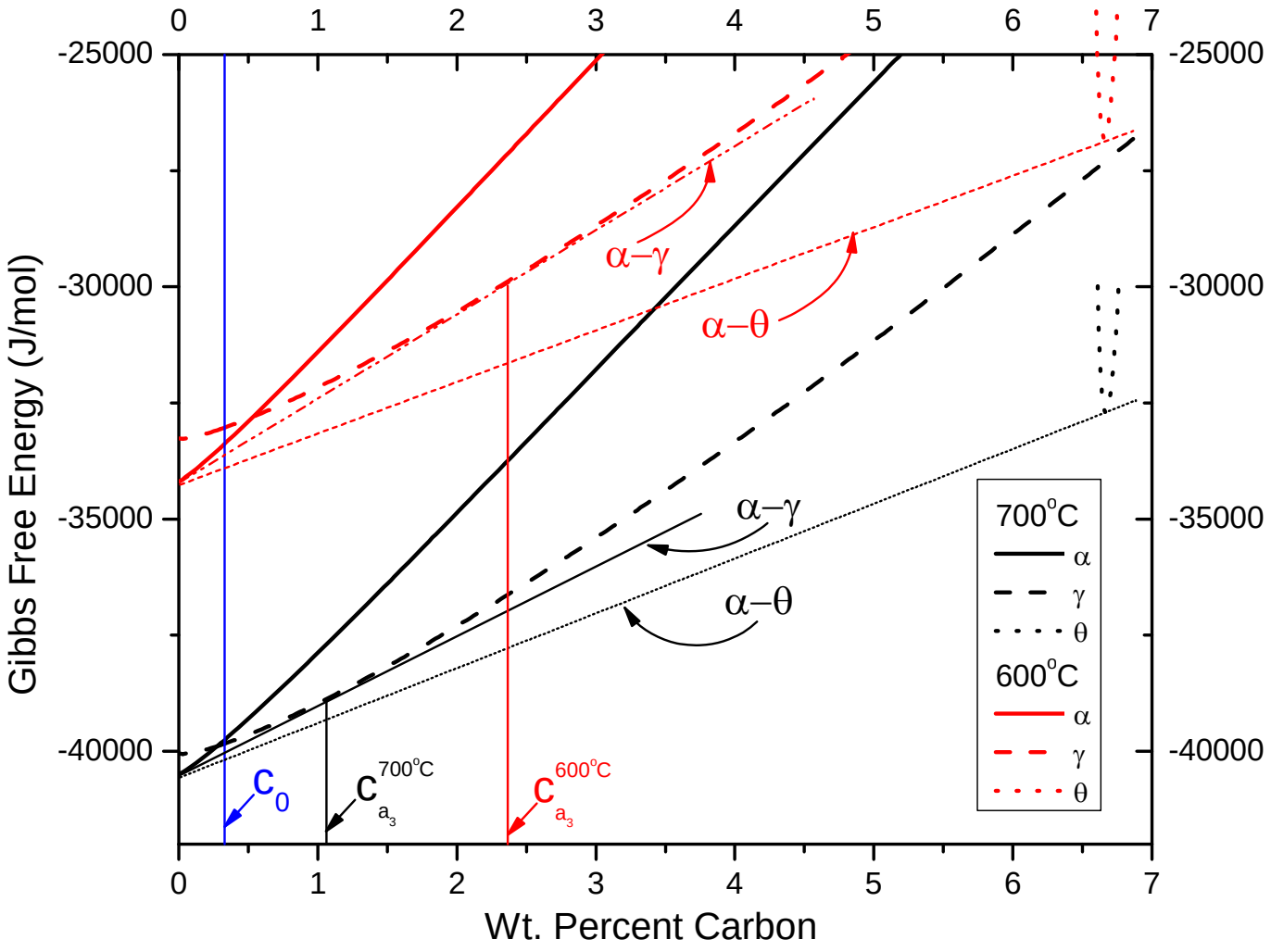

Advanced Steel Processing and Products Research Center

Driving Force for Ferrite Nucleation and Growth

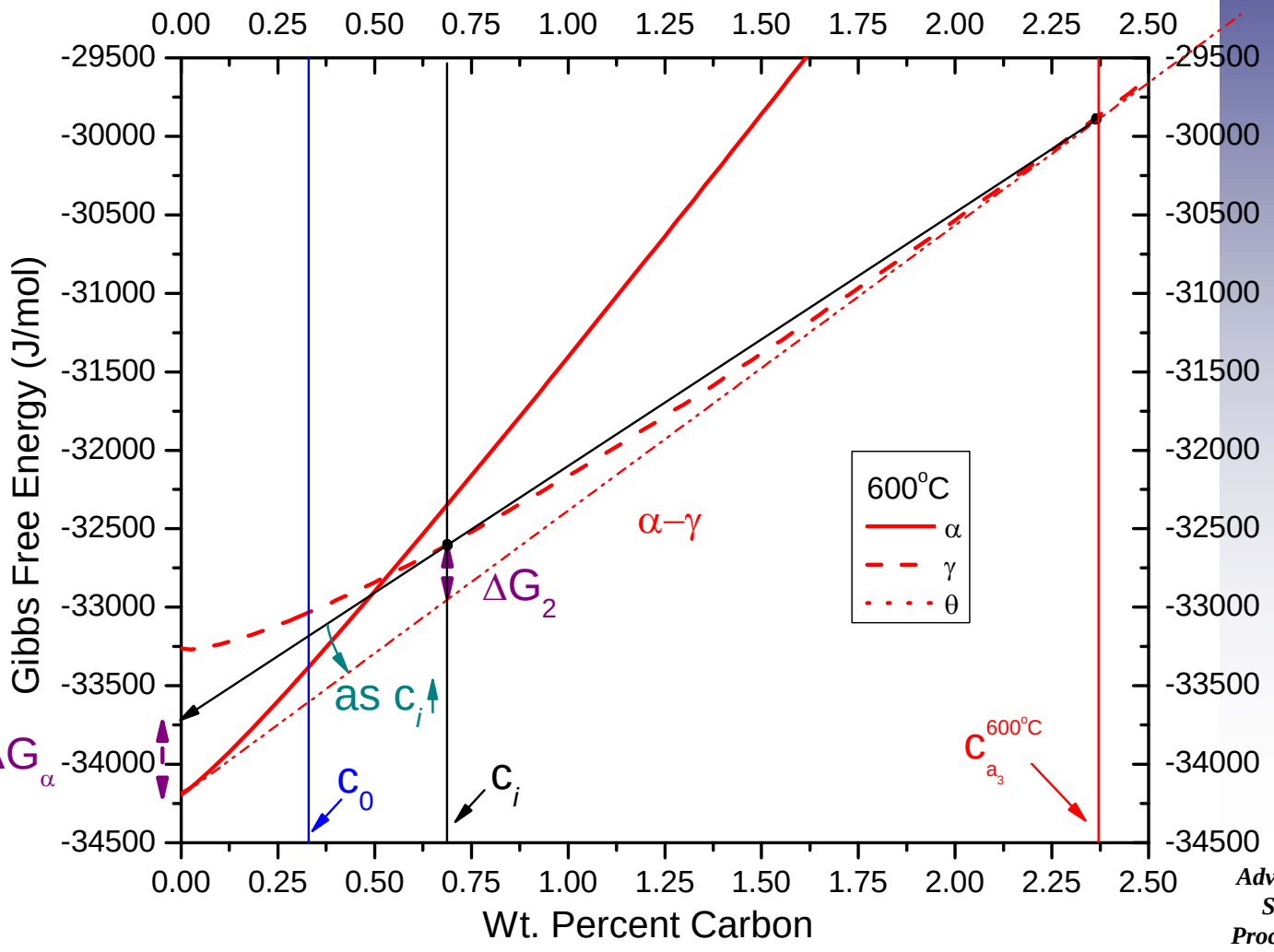

$$\Delta G_\alpha = \Delta G_2 \frac{C_\alpha - C_\gamma}{C_\alpha - C_i}$$

ΔG$_\alpha$

Ferrite Driving Force

TIMKEN

Driving Force for Cementite Nucleation and Growth

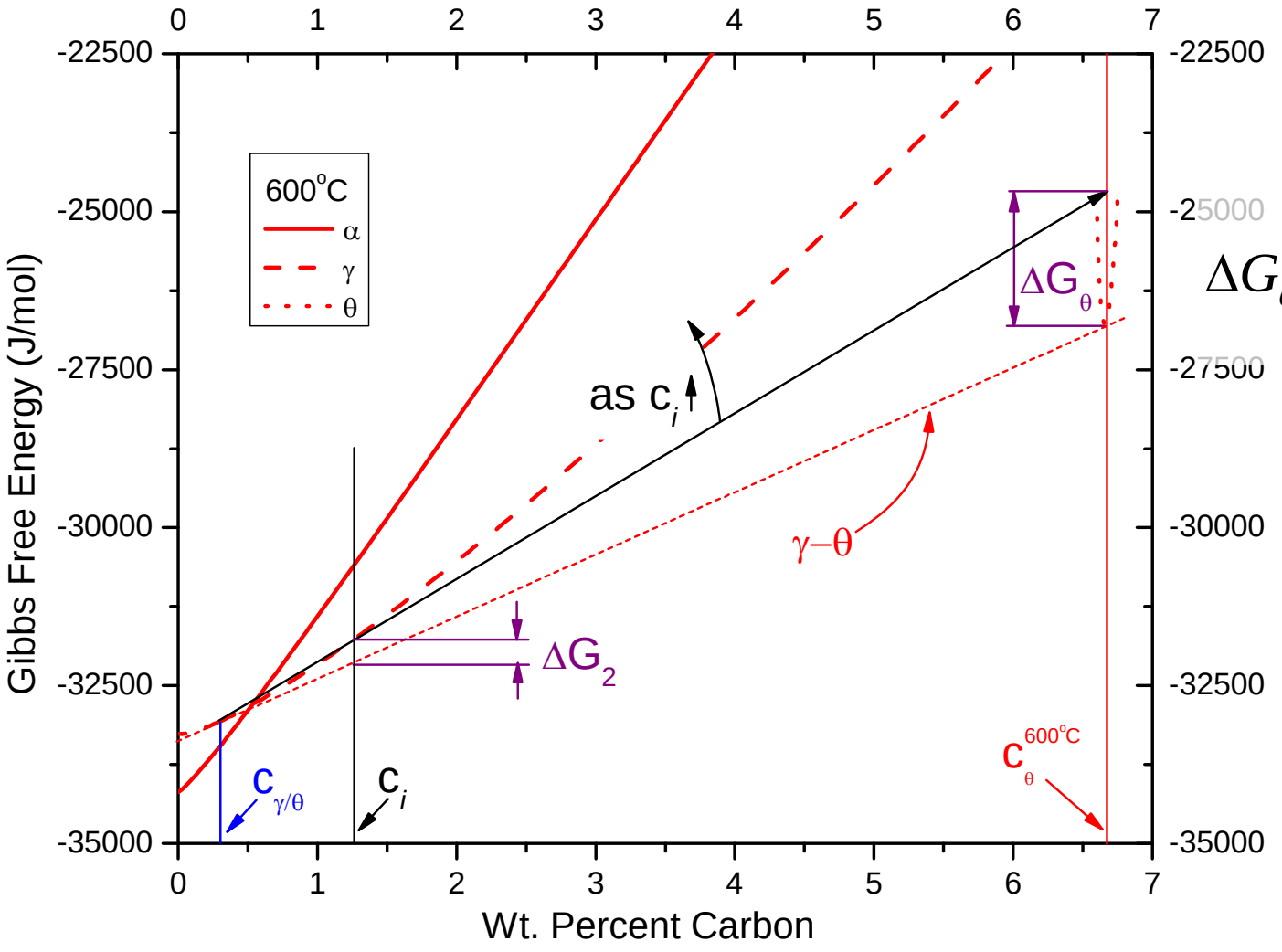

$$\Delta G_\theta = \Delta G_2 \frac{C_\theta - C_\gamma}{C_\gamma - C_i}$$

TIMKEN

Fe-0.3C Cooled at 0.05˚C/s Down to 730˚C

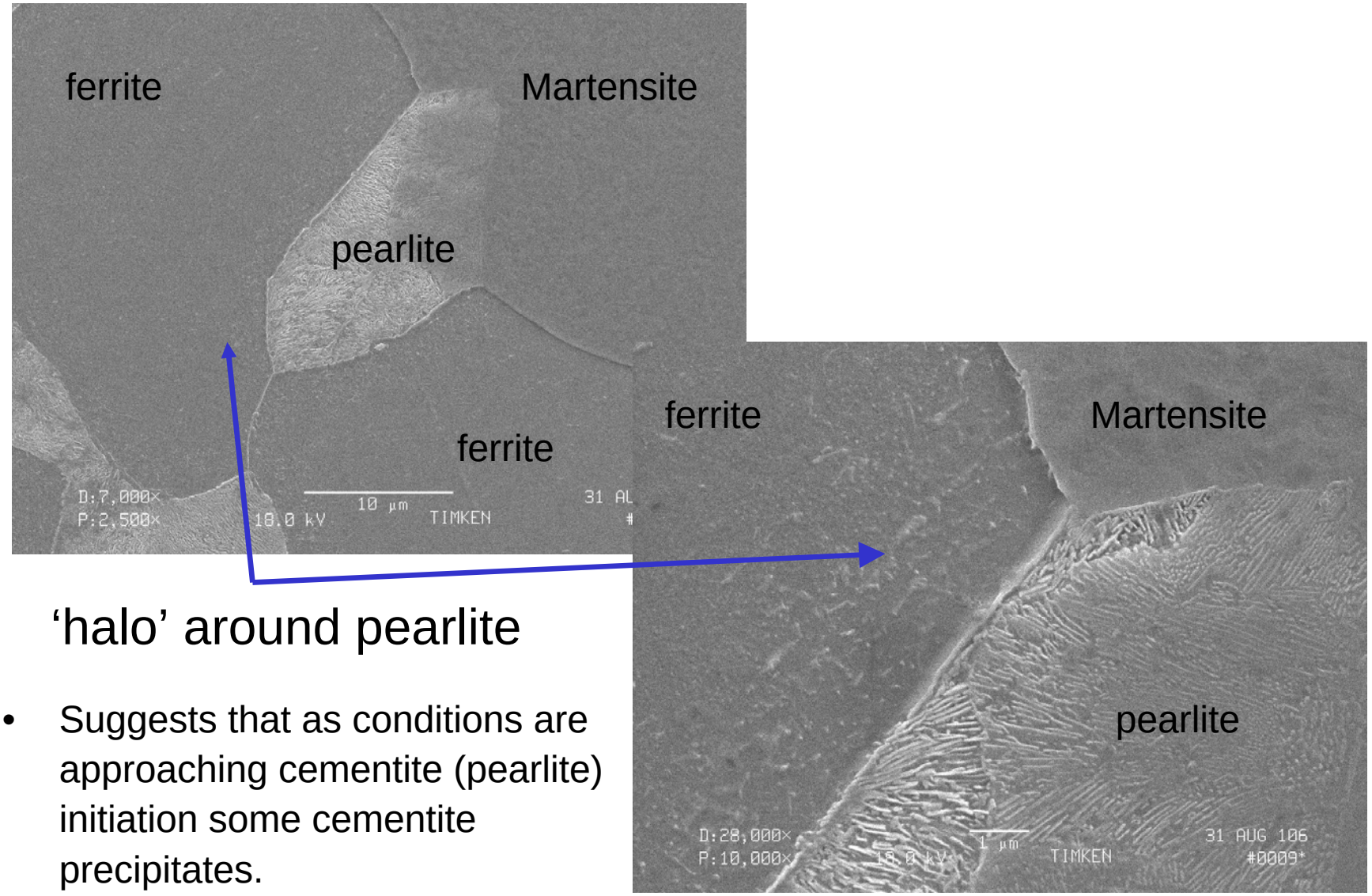

‘halo’ around pearlite

- Suggests that as conditions are approaching cementite (pearlite) initiation some cementite precipitates.

The Phase Field Method

- The derivation of the phase field equations is consistent with thermodynamic and kinetic principles.
- The derivation results in coupled partial differential equations (PDE's).
- Coupling occurs due to thermodynamic stability as a functions of local chemistry for the non-conserved (phase) field, and the thermodynamic driving force for diffusion for the conserved (composition) field.
- Solve coupled PDE's for conserved and non-conserved field variables

TIMKEN

Phase Field Method Governing Equations

Conserved Fields (i.e., composition)

$$\frac{\partial c(\mathbf{r},t)}{\partial t} = -\nabla \bullet \mathbf{J} \qquad \text{Cahn-Hilliard} \quad \mathbf{J} = -M\nabla\mu$$

$$\mu = \frac{\delta F_{cg}}{\delta c} = \frac{\delta F_{\text{chem}}}{\delta c} + \frac{\delta F_{\text{elast}}}{\delta c} + \frac{\delta F_{\text{inter}}}{\delta c} + \ldots$$

Non-Conserved Fields (i.e., phases)

$$\frac{\partial \eta(\mathbf{r},t)}{\partial t} = -L\frac{\delta F_{cg}}{\delta \eta(\mathbf{r},t)}$$

Cahn-Allen, or Time Dependant Ginzburg-Landau

My System

$$c_1 = Fe, c_2 = C, c_3 = Mn \ldots$$

$$\eta_1 = \gamma, \eta_2 = \alpha, \eta_3 = \theta, \eta_4 = ASTM \ldots$$

Advanced Steel Processing and Products Research Center

The Phase Field Method

"After selecting the field variables, the next step is to formulate the coarse-grained free energy as a functional of these fields. A general form of the polynomial approximation of the bulk chemical free energy can be written as a Taylor expansion series."

Ref. Y. Wang, L.-Q. Chen, *Methods in Materials Research* (2000) 2a.3.1-2a.3.23

Application to Fe-C system for massive and Widmenstatten ferrite has been completed

Ref. Loginova et. al. Acta. Met. 2003, p 1327-. and 2004, p 4055-.

Free Energy Contributions

Bulk free energy

$$g(\phi) = \phi^2(1-\phi)^2$$

$$p(\phi) = \phi^3(6\phi^2 - 15\phi + 10)$$

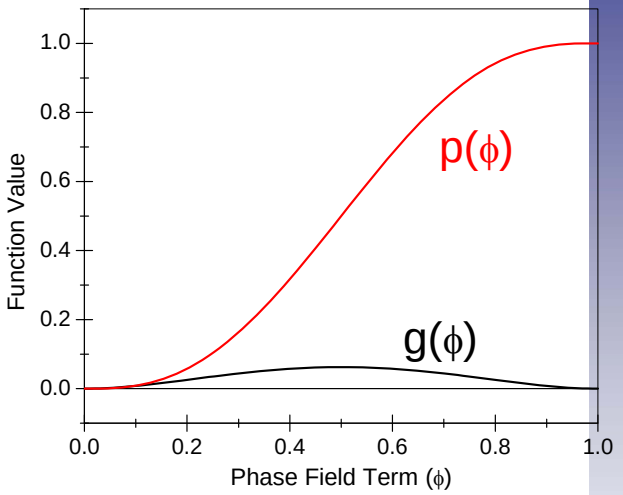

Non-conserved phase field equation

$$F_{chem} = \int_V \left[G_m(u_c, T, \phi) + \frac{\varepsilon_\phi^2}{2} |\nabla \phi|^2 \right] dV$$

Free Energy

$$G_m(u_c, T, \phi) = (1 - p(\phi))G_m^\gamma(u_c, T) + p(\phi)G_m^\alpha(u_c, T) + g(\phi)W$$

where W is a function of interface energy and thickness

and G_m is differentiable w.r.t ϕ

Non-conserved phase field

Phase Evolution Equation

$$\dot{\phi} = -M_{\phi}\frac{\delta G_m}{\delta \phi}$$

$$\dot{\phi} = -M_{\phi}\left[\frac{1}{V_m}\frac{\partial G_m}{\partial \phi} - \varepsilon^2\nabla^2\phi\right]$$

Where ε, the gradient energy term, is a function of interface energy and thickness

and M_{ϕ} is the apparent phase field interfacial mobility

Diffusion Terms

Flux

$$J_c = -L'' \frac{\partial^2 G_m}{\partial u_c^2} \nabla u_c - L'' \frac{\partial^2 G_m}{\partial u_c \partial \phi} \nabla \phi$$

$$L'' = \frac{u_c}{V_m} y_{va} M_c$$

Postulates for continuous spatial functions

Site fraction and carbon mobility

$$u_c y_{va} = p(\phi) u_c \left(1 - \frac{u_c}{3}\right) + (1 - p(\phi)) u_c (1 - u_c)$$

$$M_c = (M_c^{\alpha})^{p(\phi)} (M_c^{\gamma})^{(1-p(\phi))}$$

Conserved phase field

Composition Evolution Equation

$$\dot{u}_c = \nabla\left[(M_c^{\alpha})^{p(\phi)} (M_c^{\gamma})^{(1-p(\phi))} \left\{ p(\phi) u_c \left(1 - \frac{u_c}{3} \right) + (1-p(\phi)) u_c (1-u_c) \right\} \frac{1}{V_m} \left(\frac{\partial^2 G_m}{\partial u_c^2} \nabla u_c + \frac{\partial^2 G_m}{\partial u_c \partial \phi} \nabla \phi \right) \right]$$

Solve the coupled PDE's for $\dot{u}_c$ and $\dot{\phi}$